Clim. Past Discuss., doi:10.5194/cp-2015-165, 2016
Manuscript under review for journal Clim. Past
Published: 14 January 2016

Climate of the Past
Discussions
Open Access

An interactive tool for navigation within a database of water and carbon stable isotope records from natural archives

T. Bolliet[1], **P. Brockmann**[1], **V. Masson-Delmotte**[1], **F. Bassinot**[1], **V. Daux**[1], **D. Genty**[1], **A. Landais**[1], **M. Lavrieux**[2], **E. Michel**[1], **P. Ortega**[3], **C. Risi**[4], **D. M. Roche**[1], **F. Vimeux**[1,5], and **C. Waelbroeck**[1]

[1]Institut Pierre Simon Laplace/Laboratoire des Sciences du Climat et de l'Environnement (IPSL/CEA-CNRS-UVSQ UMR 8212), Gif-sur-Yvette, France
[2]Eawag, Swiss Federal Institute of Aquatic Science and Technology, Überlandstrasse 133, 8600 Dübendorf, Switzerland
[3]Laboratoire d'Océanographie et du Climat: Expérimentations et Approches Numériques (LOCEAN) Université Pierre et Marie Curie, 4 Place Jussieu, 75252 Paris, France
[4]Laboratoire de Météorologie Dynamique (LMD), place Jussieu, 75252 Paris CEDEX 05, France
[5]Institut de Recherche pour le Développement (IRD), Laboratoire HydroSciences Montpellier (HSM), UMR 5569 (CNRS-IRD-UM1-UM2), 34095 Montpellier, France

Received: 19 October 2015 – Accepted: 6 November 2015 – Published: 14 January 2016

Correspondence to: T. Bolliet (timothe.bolliet@lsce.ipsl.fr)

Published by Copernicus Publications on behalf of the European Geosciences Union.

Title Page
Abstract | Introduction
Conclusions | References
Tables | Figures
|◀ | ▶|
◀ | ▶
Back | Close
Full Screen / Esc
Printer-friendly Version
Interactive Discussion

Abstract

Past climate is an important benchmark to assess the ability of climate models to simulate key processes and feedbacks. Numerous proxy records exist for stable isotopes of water and/or carbon, which are also implemented inside the components of a growing number of Earth system model. Model-data comparisons can help to constrain the uncertainties associated with transfer functions. This motivates the need of producing a comprehensive compilation of different proxy sources. We have put together a global database of proxy records of oxygen (δ^{18}O), hydrogen (δD) and carbon (δ^{13}C) stable isotopes from different archives: ocean and lake sediments, corals, ice cores, speleothems and tree-ring cellulose. Source records were obtained from the georeferenced open access PANGAEA and NOAA libraries, complemented by additional data obtained from a literature survey. About 3000 source records were screened for chronological information and temporal resolution of proxy records. Altogether, this database consists of hundreds of dated δ^{18}O, δ^{13}C and δD records in a standardized simple text format, complemented with a metadata Excel catalog. For coherency with the Paleoclimate Modelling Intercomparison Project (PMIP), we focus on records spanning the past 200 years, the mid-Holocene (MH, 5.5–6.5 ka; calendar kilo years before 1950), and the Last Glacial Maximum (LGM, 19–23 ka), and those spanning the last interglacial period (LIG, 115–130 ka). For the LGM, a quality control flag was implemented to describe age markers and inform on chronological uncertainty. Basic statistics have been applied to characterize anomalies between these different periods. Most changes from the MH to present day, and LIG to MH appear statistically insignificant. Significant global differences are reported from LGM to MH with regional discrepancies in signals from different archives and complex patterns. This compilation effort highlights the need to homogenize the format of datasets and chronological information, and enhance the distribution of published datasets that are currently highly-fragmented and scattered. We also provide an online portal with an intuitive and interactive platform (http://climateproxiesfinder.ipsl.fr/), allowing one to easily select, visualize and down-

load subsets of the homogeneously-formatted records that conform this database, following a choice of search criteria, and to upload new datasets.

1 Introduction

In the context of increasing anthropogenic greenhouse gas emissions, exploring future climate change risks relies on climate models (IPCC AR5, 2013), and it becomes essential to assess their intrinsic skills and limitations (Braconnot et al., 2012; Flato et al., 2013).

Past climate was the result of the changing natural external forcings, and internal climate variability. Quantitative records of past climate variations therefore provide unique benchmarks against which is it possible to assess the ability of climate models to resolve the processes at play (e.g. Braconnot et al., 2012; Schmidt et al., 2014). However, evaluating climate models against paleoclimate data remains challenging, due to uncertainties on both simulations and reconstructions (Masson-Delmotte et al., 2013; Flato et al., 2013). On the one hand, uncertainties associated with the simulation of past climates are related to changes in boundary conditions (e.g. ice sheet topography and melt fluxes, https://pmip3.lsce.ipsl.fr/) and dust radiative feedbacks (Rohling et al., 2012). On the other hand, uncertainties also arise from the age scales of proxy records, and from the application of transfer functions used to convert proxy records into climate variables. For instance, while δ^{18}O is used as a temperature proxy in polar ice cores, the relationship between ice core δ^{18}O and temperature is known to vary trough time and between drilling sites (Masson-Delmotte et al., 2011a; Guillevic et al., 2013; Buizert et al., 2014). Similarly, the relationship between δ^{18}O from tree rings cellulose and climate may be impacted by several factors, including local monthly or annual temperature and precipitation, while the response of trees to climate changes may differ according to inherent physiological differences of the various tree species (Stuiver and Braziunas, 1987; McCarroll and Loader, 2004).

In order to constrain the second source of uncertainty, a growing number of components of climate models are being implemented with the explicit simulation of tracers such as water and carbon stable isotopes. Since the pioneer work of Joussaume et al. (1984), many models are being equipped with δ^{18}O, δD and also δ^{17}O water isotopes, including land surface models (Yoshimura et al., 2006; Henderson-Sellers et al., 2006), regional atmospheric models (Sturm et al., 2010) general circulation models (Schmidt et al., 2007 for the coupled ocean–atmosphere GISS model; Lee et al., 2008 for NCAR CAM2; Tindall et al., 2009 for HadCM3; Risi et al., 2010 for LMDZ4; Werner et al., 2011 for ECHAM5wiso; Yoshimura et al., 2011 for IsoGSM) as well as intermediate complexity climate models (Roche et al., 2013 for iLOVECLIM). Similarly, carbon stable isotopes are also implemented in a growing number of land surface and ocean components (e.g. Tagliabue et al., 2009; Menviel et al., 2012; Sternberg et al., 2009). These new functionalities of climate models open the possibility to directly comparing the proxies measured in natural archives with model outputs, with the double interest of improving the understanding of proxy records, and model evaluation. For instance, Risi et al. (2010) evaluated LMDZ4 performance against oxygen stable isotope data from terrestrial and ice archives for the MH and LGM, and Oppo et al. (2007) compared the GISS Model-E outputs with Pacific marine δ^{18}O records encompassing the MH. Recently, Caley and Roche (2013) have focused on the difference between the LGM and the Late Holocene (last 1000 years) for the comparison of the simulation from the iLOVECLIM model and proxy data, and selected 17 polar ice core records, 10 speleothems, and 116 deep sea cores with a test on age control following the protocol previously applied for the synthesis of temperature reconstructions by the Multiproxy Approach for the Reconstruction of the Glacial Ocean surface (MARGO) collaborative effort (Waelbroeck et al., 2009). Also, Jasechko et al. (2015) compiled 88 isotope records from ground water, speleothems and ice cores spanning the period from the LGM to the Late Holocene and compared these data to five general circulation models. These model-data comparisons have only used limited information extracted from

Title Page
Abstract | Introduction
Conclusions | References
Tables | Figures
◂◂ | ▸▸
◂ | ▸
Back | Close
Full Screen / Esc
Printer-friendly Version
Interactive Discussion

a fraction of available proxy records, while much broader information has been accumulated during decades of field and laboratory work worldwide.

The main open-access databases are hosted on the NOAA (http://www.ncdc.noaa.gov/data-access/paleoclimatology-data) and PANGAEA (http://www.pangaea.de) websites. These multi-proxy online data depositories are continuously updated with recent datasets uploaded by the respective authors on a voluntary basis. In some cases, datasets are also available as Supplement to publications, and practices depend on communities. For instance, there is no standard practice for archiving the growing number of stable isotope records obtained from tree ring cellulose, even though some efforts emerged recently to create a data bank (Csank, 2009). Although the two depositories have been intensively used by scientists to archive and distribute their datasets, the systematic exploration of these records remained limited by the heterogeneity of reporting, data formats including chronological information, and the impossibility to easily download all the datasets related to one type of proxy. Moreover, these databases have limited interactivity. The lack of features allowing an online pre-visualization of selected datasets obliges the users to download the data if they want to assess the relevance of the records for their scientific questions (e.g. to explore the resolution of the records, or the quality of the chronology for a given time interval). Altogether, unintuitive ergonomics and/or limited interactivity make data browsing and gathering fastidious.

Based on this observation, we decided to produce a compilation of existing records, standardising the chronological information (age markers) into a common format, and implementing an online tool to facilitate the search process throughout different archives with intuitive data browsing, online functions for datasets graphical pre-visualization, as well as easy download features. In a first step, we focus here on δ^{18}O, δD and, if available on the same archive, δ^{17}O and δ^{13}C. This choice is motivated by the following reasons: (i) these proxies have been widely used during the last decades, (ii) they are available for a variety of marine, ice and terrestrial archives (sediments, speleothems, ice and tree-ring cellulose), and (iii) they trace interactions between different components of the climate system involved in the global water and carbon cycles, and provide therefore integrated signals for evaluating respectively water and carbon cycle processes within climate simulations. A strong motivation for this compilation is the integratation of marine and terrestrial records (Bar-Matthews et al., 2003; Hughen et al., 2006; Cruz et al., 2006; Leduc et al., 2009; Carré et al., 2012; Bard et al., 2013; Grant et al., 2012, 2014). It is also in line with ongoing efforts to build consistent chronologies for marine and ice core records (e.g. the INTIMATE project, see Blockley et al., 2012). In order to document the four dimensional structure of ocean circulation changes, we included datasets from deep-sea sediments, using both surface and deep water proxies.

While in principle our methodology could allow one to explore transient climatic changes (Marcott et al., 2013; Shakun et al., 2012), such an approach would require an accurate assessment of age scale uncertainties, which is beyond the scope of this work. In our data search, we therefore focus on records providing sufficient age control and resolution for selected time slices, chosen for consistency with the Paleoclimate Modelling Intercomparison Project (PMIP), and for which numerous source records are available. The selection of target periods is described in Sect. 2. The protocols and methods used to build the database are then depicted in Sect. 3, followed by the description of the software developments required for the online search and visualization platform (Sect. 4). For the four considered time slices, we then illustrate the data coverage and spatial distributions (Sect. 5). Conclusions provide recommendations to facilitate such data syntheses, and propose future database developments.

2 Selection of target periods

Our data synthesis is focused on key periods for which there is a specific interest in the paleoclimate modeling community: the last 200 years, the Mid-Holocene (MH; 6 ka), the Last Glacial Maximum (LGM) and the last interglacial period (hereafter LIG).

The last 200 years (1800 to 2013 CE, Common Era) have been selected because (i) they encompass instrumental measurements (precipitation or seawater isotopic composition, air and water temperature, rainfall, sea level pressure. . .), and because (ii) isotopic atmospheric models can be nudged towards atmospheric historical reanalyses, thus providing a realistic framework for model-data comparisons (e.g. Yoshimura et al., 2008). It is here in fact extended back to 1800 to encompass, if possible, the climate response to the large 1809 and 1815 volcanic eruptions. This period is particularly important for detection and attribution of climate change, and, so far, the short duration of isotopic measurements in precipitation samples (i.e. at best 60 years for δ^{18}O in central Europe; Araguas-Araguas et al., 2000; GNIP Database, IAEA/WMO, 2015), has limited systematic investigation of recent trends. Here, we aim at expanding this documentation from highly-resolved proxy archives (mostly ice cores and tree-ring cellulose). Note that the records do not necessarily span the entire key periods (i.e. a record spanning only the last 50 years would be included in our statistics for the present-day period).

The MH (6 ± 0.5 ka, thousand years before 1950) has been selected as a target for paleoclimate modeling (https://pmip3.lsce.ipsl.fr) as a compromise between the magnitude of orbital forcing, and climate responses at the end of the glacial ice sheet decay. The orbital configuration produces enhanced (reduced) insolation in the northern (southern) hemisphere during boreal (austral) summer, associated with warming in mid and high Northern Hemisphere latitudes as well as enhanced Northern Hemisphere monsoons (Braconnot et al., 2012). So far, most quantitative model-data comparisons for this period have focused on sea surface (Hessler et al., 2014) or surface air temperature inferred from marine and pollen data, and precipitation changes inferred from pollen or lake level data (Harrison et al., 2013). They suggest that models tend to underestimate the magnitude of latitudinal temperature gradients, as well as the magnitude of continental precipitation changes (Flato et al., 2013). While the signal-to-noise ratio is often small, this recent period is well documented in many well-dated, high-resolution archives, motivating a synthesis of proxy information.

The LGM (19–23 ka) corresponds to a major global climate change, in response to decreased greenhouse gas concentration and expanded continental ice sheets, with an amplitude of global cooling of around 4 °C, comparable to the magnitude of projected 21st century high-end warming (Collins et al., 2013). Due to the magnitude of the radiative perturbation associated with changes in atmospheric composition and ice sheet albedo, this period is particularly relevant for climate sensitivity (Masson-Delmotte et al., 2013; Rohling et al., 2012; Schmidt et al., 2014). Moreover, the LGM has been widely investigated through well-preserved natural archives with improved chronologies (Reimer et al., 2013). A synthesis of marine data has been achieved within the MARGO collaborative effort (Waelbroeck et al., 2009), leading to a database of multi-proxy sea surface temperature estimates, complementing surface air temperature change between the LGM and present-day inferred from pollen and ice core records (Braconnot et al., 2012). This period is marked by changes in the thermohaline circulation (Duplessy et al., 1988; Shin et al., 2003; Yu et al., 1996), large scale atmospheric circulation (Chylek et al., 2001; Justino and Peltier, 2005; Murakami et al., 2008), El Niño–Southern Oscillation (ENSO; Tudhope et al., 2001; Stott et al., 2002) as well as the monsoon and Inter-Tropical Convergence Zone (ITCZ) position (Van Campo, 1986; Braconnot et al., 2000; Broccoli et al., 2006; Leduc et al., 2009; Bolliet et al., 2011; Sylvestre, 2009). The large uncertainties associated with changes in ocean circulation and their role for the carbon cycle and the tropical water cycle have already motivated data syntheses and model-data comparisons (Bouttes et al., 2012; Caley et al., 2014; Risi et al., 2010).

Finally, the last interglacial period (115–130 ka) is characterized by large changes in orbital forcing, together with reduced volume of the polar ice sheets (Kukla et al., 2002; Govin et al., 2012; Masson-Delmotte et al., 2013; Capron et al., 2014). While global mean temperature is estimated to be less than 2 °C warmer than today, based on syntheses of temperature reconstructions and simulations (Otto-Bliesner et al., 2013), Northern Hemisphere summer warming in this period can reach the same magnitude of feedbacks than in future projections (Masson-Delmotte et al., 2011a). It is also characterized by enhanced inter-hemispheric and seasonal contrasts (Nikolova et al., 2013). Large uncertainties also reside on the conversion of Greenland and Antarctic ice core water stable isotope records to temperature, with implications for assessing the vulnerability of ice sheets to local warming (Masson-Delmotte et al., 2011a; Sime et al., 2009, 2013; NEEM community members, 2013). Climate models have been shown to underestimate the magnitude of Arctic warming and to fail capturing Antarctic temperature trends (Lunt et al., 2013; Bakker et al., 2014). This may arise from vegetation and land ice feedbacks, which were not resolved in the simulations. While all of the above motivate a proxy record synthesis for this period, highly-resolved archives remain scarce (Pol et al., 2014), and large age-scale uncertainties constitute a major obstacle, especially given the asynchronous climate change detected in both hemispheres (Stocker, 1998; Masson-Delmotte et al., 2010; Bazin et al., 2013; Capron et al., 2014).

3 Database construction steps

The first step consisted in gathering all the δ^{18}O, δ^{13}C and δD data available from the two main online paleoclimate data depositories (NOAA and PANGAEA), together with marine sediment records from the LSCE (Gif-sur-Yvette, France), paleoceanography internal database (Caley et al., 2014) and literature survey and personal communication (2013, 2014) with authors. This work was performed from May 2013 to July 2014.

A metafile has been built in order to list the main parameters of these datasets: core name, reference, associated publication Digital Object Identifier (DOI), core site latitude, longitude and elevation or depth coordinates. We have also inserted a flag to describe the quality of age models for marine sediment cores (see next section). All ages were converted into thousand years before present (ka), using 1950 CE as the reference year. For each archive, we have stored the depth/age/proxy value data into a separate three-column file. This protocol was applied to each archive and proxy record. For instance, for a publication reporting δ^{18}O time series based on four different foraminiferal species, extracted from two deep sediment cores, we have produced eight files, using a simple text tabulated standard format. This standardization was adopted in order to facilitate the comparison of records, and to allow fu-

Title Page
Abstract | Introduction
Conclusions | References
Tables | Figures
◀| |▶
◀ ▶
Back | Close
Full Screen / Esc
Printer-friendly Version
Interactive Discussion

ture automated calculations. The name of this standard data file was inserted into the metafile. The name of output files was established based on the name of the original file provided by authors. We thus simply added the acronym “SIMPL” (for “simplified”) to the data-only file name. For publications presenting several records, the different cores, species and/or proxies were indicated to the individual data files. For instance, “stott2007_MD81_cmund_corrected_SIMPL” and “Stott2007_MD81_cmund_SIMPL” are the output files for the δ^{18}O records from core MD98-2181 published by Stott et al. (2007), based on the benthic foraminifera *Cibicidoides mundulus* with and without adjustment for vital effect, respectively.

All the available information describing the associated age model was extracted and compiled into a separate spreadsheet named after the original data file, with the addition of the “TIEPTS” (for “tie points”) to the file name, as well as the core reference in case of articles based on multiple records. This spreadsheet contains sample reference and depth, raw and/or calendar ages from radiometric dating with the name of the species or the type of material measured, tie points used for core-to-core correlation, and the amount of dated material. The name of this file was also listed in the metafile, and this information was used to evaluate the age model (see next section).

This database was used to calculate basic statistics (number of data points, average proxy value, standard deviation) for the MH, the LGM, the last Interglacial, and for the reference present-day climate (last 200 years).

4 Age model evaluation

4.1 Deep sea sediment cores

Following the protocol developed for the MARGO project (Waelbroeck et al., 2009), quality flags were attributed to the chronology of the deep sea sediment cores and speleothems. For this purpose, several factors were taken into account:

1. The density of chronologic markers: AMS ^{14}C and/or U-Th dates, core-to-core correlation tie points, reference horizons (tephra, paleomagnetic excursions...).
2. The position of age markers, especially at the boundary of our target periods. For instance, we consider that the LGM (19–23 ka) is better constrained with two AMS ^{14}C dates at 19 and 23 ka than with four dates within the 20–22 ka interval.
3. The presence of sedimentary disturbances (turbidites, hiatus, bioturbation) and post-deposition or coring events (gaps, core breaks, post-depositon reorganization of speleothems crystals). This aspect of the age-model evaluation is however restricted to the information provided by authors concerning the eventual presence of such disturbances.
4. The level of detailed description of the age model: raw ^{14}C and U-Th ages, samples reference, type of material or species analyzed, reservoir age and calibration program or curve used in case of marine material. Reservoir ages still remain vigorously discussed (Soulet et al., 2011; Siani et al., 2013). Here, we used the reservoir ages as originally published.
5. Marine Core-top constrains. It is customary among paleoceanographers to assign “0 BP” to the uppermost sample of the core. Many late Holocene records are also dated using extrapolated ages between the most recent datum and the top of the core. This implies that the top of deep-sea cores is often poorly chronologically constrained. Although arbitrarily dated, these data points were integrated to the calculation of present-day average values.
6. For records older than the ^{14}C reliability interval (~ 35 to 60 ka, where the uncertainty on the calibration into calendar ages strongly increases, Plastino et al., 2001; Bronk-Ramsey et al., 2013), the quality flags are based on the number of tie points, and the type of material used for core-to-core correlation (e.g.: well dated high resolution ice core vs. low resolution sediment core).

Quality flags ranging from 1 (very good) to 5 (poor) were therefore included in the metafile for each deep-sea sediment core and speleothem dataset. This evaluation protocol was not applied to archives such as tree rings, varved lacustrine cores, high accumulation ice cores, modern corals or mollusk shells where annual counting allows building accurate chronologies. We thus assigned the best quality flag to these records.

In order to illustrate the chronological quality flag, we describe hereafter five examples:

a. Quality Flag 1 (excellent): Marine Core A7 (27.82° N, 126.98° E investigated by Sun et al., 2005) is constrained by 15 well-distributed AMS ^{14}C dates ranging from 1 to 17.5 ka, corresponding to the time period where oxygen stable isotope data are available. There is therefore no significant arbitrary-dated interval. The authors used a dated ash layer to establish a precise correction of the theoretical reservoir age, and the effect of local turbidites was precisely monitored. The dating protocol is described in detail, and reports samples labels, reservoir age, and the calibration curve. Despite the lack of information on the selected species and the amount of material used for ^{14}C dating, we assigned the maximum quality flag to this age model.

b. Quality Flag 2 (good): Marine Core GEOB3129/3911 (4.61° S, 36.64° W) is dated through 16 AMS ^{14}C dates spanning the 1.8–20 ka interval, which coincides with the period covered by isotope measurements (Weldeab et al., 2006). The dating protocol is relatively well described although reservoir ages and the amount of measured material are not directly mentioned. With one date at 20 ka and another one at 16.9 ka, the distribution of dates does not provide a precise picture of the timing of the starting date of the last deglaciation.

c. Quality Flag 3 (average): Marine Core KNR159-5-33GGC (27.56° S, 46.18° W; Tessin and Lund, 2013) is constrained by 14 AMS ^{14}C dates between 1.6 and 18.5 ka, and the entire dating protocol is well described. However, the AMS ^{14}C dates are not homogenously distributed, with only 4 data points within the 1.6–

14 ka interval and 10 dates between 15.4 and 18.5 ka. The chronology of the Holocene is therefore poorly constrained. Moreover, anomalously old material is intercalated between younger sediment, interpreted as deep burrying (Sortor and Lund, 2011).

d. Quality Flag 4 (below average): the age scale of Core RC10-196 (54.70° N, 177.08° E) is particularly well described by Kohfeld and Chase (2011). However, only three AMS ^{14}C dates and one δ^{18}O data point for oxygen isotope stratigraphy are available between 10 and 22 ka, while the δ^{13}C and δ^{18}O records span a considerably wider time interval (10–86 ka). The starting point of Termination I is not well defined in δ^{18}O, making the datum at 22 ka relatively imprecise. Although the authors did not focus on the last deglaciation, we incorporated this record in the database, because only very few records have been recovered in this part of the North Pacific.

e. Quality Flag (poor): δ^{18}O record from Core M44/3_KL83 (32.60° N, 34.13° E; Sperling et al., 2003) spanning the last 13 kyrs. This record is constrained by only one ^{14}C AMS date (7.6 ka), leading to large uncertainties in the timing of the whole Holocene.

4.2 Other archives

4.2.1 Ice cores

Dating ice cores is a crucial issue, as these highly-resolved archives are often compared to marine cores and speleothems to assess the timing of climatic events between high and lower latitudes. Ice core chronologies are regularly updated using available age markers and dating is synchronized among different ice cores (e.g. Rasmussen et al., 2006; Vinther et al., 2006; Ruth et al., 2007; Bazin et al., 2013; Veres et al., 2013), with estimates of associated age scale uncertainties. For that reason, it was decided not to attribute dating quality flags for ice cores chronologies in this database.

For the last interglacial period, LGM and MH, most ice cores chronologies would be flagged as good to excellent, depending on the dating strategy. For the last 200 years, the quality of ice core chronologies can vary from excellent for high accumulation areas (where annual layer counting and volcanic horizons are available) to good in the driest central Antarctic areas.

4.2.2 Speleothems

Dating speleothems generally involves radiometric methods or, in rare cases, counting of annual laminae when they are visible. In the majority of cases, it is based on uranium series methods (schematically ^{234}U decays into thorium ^{230}Th); when the U/Th method is not possible because of too large detrital content, some authors may use AMS ^{14}C with a correction of dead carbon producing quite large errors. U-Th method on speleothems can have a $< 1\,\%$ 2 s error bar and the age limit of the method is close to 450 ka; but depending on the detrital content of the calcite and on the method used (i.e. TIMS, MC-ICPMS or alpha counting for old records), errors may be variable. Chronologies based on radiometric dating were evaluated similarly to what was done with marine cores, with quality flags based on the resolution and distribution of the dated samples, and taking into account the possible sedimentary issues (recrystallizations, hiatus not caused by climate fluctuations). In the case of dating by lamina counting, similarly to what was done to modern coral records, we considered that the error on the chronology is low, and assigned the maximum quality flag to the age model of these cores.

4.2.3 Lacustrine records

The construction of age models for lacustrine cores is somewhat similar to what is applied for marine cores. Most of the chronologies are based on AMS ^{14}C dating measured on carbonate or organic compounds. Similarly to what was performed for marine datasets, the quality flags for lacustrine records are based on the density of ^{14}C dates and their position relatively to key transitions. We also took the sedimentary disturbances (e.g. sedimentation hiatuses) into account as well as the presence of eventual corrections for residence time and reservoir effects revealing an effort for considering the impact of the lake circulation dynamics in the sediment age.

The chronology of some of the compiled lacustrine records was performed by counting of seasonal varve, generally resulting in a high accuracy (Sprowl, 1993). As a result, we attributed the “excellent” quality flag to varve-based chronologies.

4.2.4 Tree-ring records

Tree-ring are generally short and well-dated records. The dating method is based on precise counting of single rings produced each year by individual trees. Although some chronologies can be affected by few double or missing rings, tree-rings may be the archive presenting the most robust chronologies and allow the attribution of a precise calendar year to each of the rings. We therefore assigned the “excellent” quality flag to all of the tree-ring records of our database.

5 Interactive visualization tool

NOAA and PANGEA open-access online libraries host a huge amount of palaeoclimatic datasets, but browsing and downloading these data may sometimes not be optimal. Each dataset must indeed be downloaded individually, without having the possibility to quickly visualize the records online.

This is particularly critical when users need to download a large amount of records not corresponding to a specific site and/or author. This lead us to develop a tool that optimizes the datasets browsing step, with an online data plotting function, and a user-friendly tool for downloading multiple datasets.

One of the main aims of this new platform is the enhancement of the interactivity during the data browsing process, in comparison to the existing libraries that are, on this aspect, relatively limited. Our portal (http://climateproxiesfinder.ipsl.fr/) provides a dynamic feature that makes an inventory of the available records according to the settings defined by the user (Fig. 1). Once the type of proxy (δ^{18}O, δ^{17}O, δD, δ^{13}C) and archive (marine, lacustrine or ice cores, speleothems, tree rings) is defined by users, a feature will allow them to refine their request by (1) choosing the material (e.g. corals, planktonic or benthic foraminifera for marine records), (2) restraining the area of interest by dragging and zooming in and out of the world map, and (3) dragging the scale of core depth/elevation and time interval of interest (blue and orange plots on Fig. 1), with a real-time dynamic update on the map of the cores matching these criteria, as well as in the list of the available records. This list displays information on the records (core name, authors, time interval spanned, species used, core site latitude, longitude and depth/elevation) and also allows a direct access to records for users who already know which datasets they want to download, without browsing through the map or search engine.

Once the appropriate records are found, an online data visualization tool allows a quick and direct comparison of several selected datasets. This function constitutes a drastic improvement for palaeoclimatologists, compared to the existing online libraries, as it allows users to check and compare different records before selecting the datasets to download. Our platform then provides a multiple-dataset downloading function, targeted to climate modelers who aim at global or regional model-data comparisons.

The interface between the web page, the database metafile and the individual data files is managed by a D3 javascript engine linked to cross-filtering (dc.js and Crossfilter) and interactive mapping (Leaflet) libraries.

6 Results

The overall increase in the number of records and publications per year over the last 50 years (Fig. 2) reflects the growing investment in obtaining stable isotopes records to document and understand past climates. The peak in the number of records published in 1988 and 1994 are mostly due to the presence of some publications compiling a large number of previously unpublished marine records from the Atlantic Ocean (Sarnthein et al., 1988, 1994).

6.1 Geographical distribution of data and temporal resolution

This section briefly describes the status of the database for marine and terrestrial records (Fig. 3), and provides a synthesis of stable isotope data for each focus period.

A total of ~ 6400 records were collected from the NOAA and PANGAEA data repositories as well as from the internal LSCE database. About 3300 marine records were rejected, as they are not yet published. Following the settings of our online portal, we also isolated about 300 δ^{18}O and δ^{13}C published records not dated (~ 200 records) or containing no information about the core site elevation or depth (~ 100 records). We thus accumulated about 1700 δ^{18}O records from ~ 900 sites, about 900 δ^{13}C records from 450 sites, and about 230 δD records from 60 core sites (with 20 additional deuterium excess records). When considering the different types of archives, we compiled about 1200 δ^{18}O and ~ 700 δ^{13}C records from 600 marine sediment cores, 200 δ^{18}O and 75 δ^{13}C speleothems records from 60 caves, 200 dated δ^{18}O records from 50 ice cores (with about 60 additional dated δD datasets and a few δ^{17}O records), 60 δ^{18}O and 60 δ^{13}C lacustrine records (with δD datasets), as well as 85 δ^{18}O and 80 δ^{13}C records from tree rings.

Among all the 1900 collected marine records, about 850 do not present any information about the construction of their age model and about 950 records are associated with age model tie points or by default associated with an excellent chronology (e.g. modern corals), while most of the lacustrine cores and speleothems are associated to chronological information. We also note that, when not considering tree-rings records, about 500 dated records do not present any sampling depth or distance scale. The absence of the age scale and/or chronological tie-points clearly prevents any comparison with other records or with climate model outputs. Similarly, the absence of a depth scale prevents the detection of potential sedimentary or chronological issues, and therefore the correction with existing age models.

6.1.1 Geographical distribution

For each period of interest, although the amount of compiled records is large enough, the geographic distribution of marine cores is not homogenous, as 75 % of the δ^{18}O and δ^{13}C dated records are located in the Northern Hemisphere, with a maximum density in the northern sub-tropical band (Figs. 3 and 4). The Atlantic Ocean is the best documented (about half of all marine records). Most of the compiled records for the Indian, Pacific and Southern Oceans come from sediment cores recovered on continental margins, because a part of the seafloor in the open ocean is deeper than the carbonate compensation depth in these basins (Berger and Winterer, 1974), and the sedimentation rate is particularly low in the large oligotrophic areas of the open ocean. This lack of suitable core sites constitutes a critical limitation for the documentation of the past open-ocean circulation and mechanisms affecting the entire Indian and Pacific basins, such as ENSO, latitudinal migrations of the ITCZ, fluctuations in the thermohaline circulation, with possible formation of past North Pacific intermediate and deep water (Mix et al., 1999; Ahagon et al., 2003; Max et al., 2014), and storage of carbon in the Southern Ocean (Skinner et al., 2010; Burke and Robinson, 2011). Vast areas remain virtually undocumented in the Indian, Pacific and Southern Oceans. A large majority (about 90 %) of the records of the ocean database are based on foraminifera, while corals are much scarcer and only few studies use molluscs or diatoms.

The distribution of continental records (Fig. 3) naturally depends on the position of caves, lakes, forests as well as ice sheets and glaciers. Speleothem δ^{18}O records are found on each continent, but with a very heterogeneous distribution. In fact, due to the distribution of caves presenting exploitable speleothems, several large areas (Russia and central Asia, northern and tropical Africa, Canada, central South America) remain undocumented, while the density of records is large in Europe, USA, Central America and China. While they have provided highly resolved records of regional climate variability (e.g. the monsoon and ITCZ, circum-mediterranean continental climate), speleothems do not provide a global coverage. Lacustrine records are also very unevenly distributed, with very few dated isotopic records in South America, Africa, Russia and Australia, although these regions present numerous lakes.

Oxygen and carbon stable isotopes from tree rings cellulose have recently emerged as powerful paleoclimate proxies, albeit with heavy sample preparation (Libby et al., 1976; Long, 1982; Ehleringer and Vogel, 1993; Switsur and Waterhouse, 1998). This feature, and the fact that few tree ring isotopes datasets are available online, lead to relatively scarce archives at a global scale. Most of the available records are located in Europe, while the remaining other datasets (mainly δ^{13}C records) are restrained to a few sites in Asia, South America, Siberia, Costa Rica and USA. This distribution of records implies that associated large-scale climate reconstructions are somewhat constrained to Europe.

With respect to ice cores, 75 % of the compiled δ^{18}O and δD are from Greenland and Antarctica. Few cores indeed were recovered from high elevation ice caps and glaciers from the Andes, Alaska, Arctic Russia, Svalbard, Mount Kilimanjaro and the high-latitude Canadian islands, close to Greenland (Fig. 3). We stress the fact that most published ice core records from Tibet spanning the past centuries are not available from open-access sources.

Contrary to the geographical distribution, the vertical distribution of marine cores along the water column is relatively homogenous for the global ocean (Fig. 5), with more than 100 datasets in each of the 500 m-thick layers from the surface down to 4000 m, while data are scarce below this level.

6.1.2 Temporal distribution

We now describe the distribution of records throughout the different periods of interest (Fig. 6). Marine δ^{18}O and δ^{13}C records are well represented over the four periods, with at least 200 records available for each of the time slices. However, many marine

Title Page
Abstract Introduction
Conclusions References
Tables Figures
◀◀ ▶▶
◀ ▶
Back Close
Full Screen / Esc
Printer-friendly Version
Interactive Discussion

sediment core tops are poorly dated, and thus the number of marine data delivering a robust characterization of recent oxygen and carbon isotopic composition is limited. About half of the marine records have only one data point over the last 200 years (about 50 % of the δ^{18}O records and 60 % of the δ^{13}C records) and most of them have less than ten data points over the last 200 years (~ 65 % of δ^{18}O and δ^{13}C records). When considering the other PMIP key periods, it appears that the distribution is similar for the MH (about 90 % of the δ^{18}O and δ^{13}C records have less than ten data points), while the resolution is slightly better for the LGM (65 % of δ^{18}O and 70 % of δ^{13}C records have less than ten data points) and for the large time interval assimilated here to the last interglacial (~ 50 % records have less than ten data points).

Speleothem records span a large variety of time-intervals, ranging from seasonal to glacial/interglacial scale. Due to the heterogeneity of the time slices spanned by speleothems records, the information provided is relatively fragmented. As a result, although we compiled more than 200 speleothem δ^{18}O records, none of the four key time-slices selected by the PMIP project contains more than 60 records (30 for δ^{13}C), due to the fact that many records span time intervals are in between these time-slices. Also, only three dated speleothem δ^{18}O records span the entire time interval from the last interglacial period to present-day, and only 14 records span both the LGM and the MH. In general, speleothem records have a better temporal resolution than marine records. For each of the four key periods, at least 60 % of the records display more than ten data points. One difficulty arises from the fact that exceptionally long speleothem records such as the one obtained from the Hulu and Dongge caves records (Wang et al., 2001, 2005) have been obtained from the compilation of measurements performed on several speleothems/cores from one single cave. These multiple individual cores may present significant and varying offsets which can be identified over different periods of overlap (see Wang et al., 2001; Yuan et al., 2004). As a result, establishing a robust composite record allowing calculation of anomalies between different past periods is particularly delicate for these archives. For this reason, we decided to keep the individual short datasets separated as they were published, and did not build long and continuous composite records. Therefore, composite records cannot be displayed in our LIG-MH comparison map (Fig. 9). δ^{18}O records from ice cores are relatively scarce for the oldest PMIP time slices, with only ~ 45 records spanning the MH, ~ 40 for the LGM, and 14 concerning the LIG (13, 13 and 6 for δD, respectively). Only five δ^{18}O records are continuous from the LIG to the Holocene. Ice core records however provide a wealth of information on the spatial and temporal variability of surface snow isotopic composition over the last decades, as about 140 of the ~ 180 compiled δ^{18}O dated records spanning the last 200 years exhibit at least ten data points within this period (50 out of 55 dated records for δD and deuterium excess).

As the effect of burial on δ^{18}O of fossil wood cellulose remains poorly known (Richter et al., 2008), we selected records exclusively based on living trees or timber wood. Consequently, the compiled records from tree ring cellulose can only be used to monitor the climate fluctuations of the last millennium at the very best. We have identified ~ 80 tree ring cellulose δ^{18}O records which cover the past 200 years (~ 80 for δ^{13}C). Most of the records have been provided at seasonal to decadal temporal resolution.

Lacustrine cores are generally short and records generally span relatively limited time intervals. As a result, only the PD and MH are covered by a relatively large number of records (~ 35 δ^{18}O, 30 δ^{13}C and ~ 135 δD records for PD; 25 δ^{18}O, 30 δ^{13}C and ~ 45 δD records for MH), while datasets spanning the LGM and LIG are very scarce (30 when considering δ^{18}O, δ^{13}C and δD records).

Datasets temporal resolution

Figure A1 (see Appendix) shows the variety of temporal resolutions in the compiled records spanning the past 200 years (1800–2013 CE). Dating of marine sediment core tops remains a critical issue, due to alterations during the coring process as well as sediment reworking and bioturbation. In fact, the upper first centimetres are generally water-soaked and thus often lost or altered during the recovering of marine cores, which, in case of moderate or low sedimentation rates, leads to the loss of material spanning the last hundreds or thousands years. Additionally, bioturbation can alter the upper sediment down to 10 cm below the water–sediment interface (Boudreau, 1998). As a result, many core tops provided as present day references might actually reflect older conditions (from several centuries to few millennia, Barker et al., 2007; Löwemark et al., 2008; Fallet et al., 2012). Solving these issues might require a precise investigation of bioturbation tracks in the upper layers of sediment cores and drastic improvement of the coring and analysis techniques, as suggested by the final conclusions of Keigwin and Guilderson (2009): “Until we can directly radiocarbon date individual foraminifera, the role of bioturbation will always be a problem in core top calibration studies”. These sedimentary issues are often accompanied by insufficient resolution and quality of the sediment core-tops dating procedure. In fact, present-day conditions are represented by only one data point in about half of the datasets, generally dated via linear extrapolation of deeper tie-points. About 95 marine δ^{18}O and 35 δ^{13}C records exhibit a decadal to annual resolution, generally arising from corals (65 % of the records) with robust layer-counted annual chronology.

While chronology is not an issue for tree ring cellulose records, the number of individual tree samples combined for each year can be a limiting factor. Several studies have investigated the signal to noise ratio, and demonstrated the importance of combining at least 4–5 trees from a forest to extract the common climate signal (e.g. McCarroll and Loader, 2004; Daux et al., 2011; Labuhn et al., 2014). The same issue arises for ice core records, especially for the past centuries when the noise caused by processes such as wind scouring can be significant when compared to the small climatic signal (e.g. Fisher et al., 1985; Masson-Delmotte et al., 2015). As a result, the records resulting from stacks combining several ice cores from a given site have stronger climatic relevance than records based on individual ice cores. However, the non-polar ice cores experience their best dating on this period. The dating is usually based on the multi-proxy annual layer counting which is based on the seasonal variations of insoluble particles and the isotopic composition of ice. Moreover, the natural radioactive material decay of suitable radionuclides (Pb^{210} for example) and the identification of prominent horizons of known age from radioactive fallout after atmospheric thermonuclear test bombs (Cs^{137}, Sr^{90}, Am^{241}) provide absolute reference horizons, and are currently used in the Southern Hemisphere (Vimeux et al., 2008, 2009a for example in the Andes).

Several recent speleothem and short ice core records benefit from annual layer counting, with an accurate chronology, but this is not systematic. Ice core datasets encompass a large proportion (~ 70 %; 120 records) of highly-resolved (decadal to annual) records, while this percentage is significantly reduced for speleothems (about one half of the 90 records spanning the last 200 years).

For the MH and LGM, marine records also have the lowest temporal resolution, as 80 % of these datasets exhibit 4 data points or less over the 5.5–6.5 ka interval, and none of the records are available with a resolution better than respectively 20 and 40 years (Figs. A2 and A3 in Appendix). Ice core records spanning the MH and the LGM are relatively scarce (55 and ~ 50 datasets, respectively), and most of them exhibit decadal to centennial resolution. Speleothem records are slightly more abundant than ice core records (90 and 55 records for the MH and the LGM, respectively), with very variable resolution, from millennial to sub-decadal. Speleothems and ice core records spanning the Last Interglacial are scarce (about 35 and 15 records, respectively; Fig. A4 in Appendix) and only some of them present a centennial resolution or better, while marine records are abundant, but most of them have millennial or lower temporal resolution.

Lacustrine data can roughly be divided into two groups, with about half of the records covering only the last decades, while the other records are generally much longer, spanning the Holocene period, and few datasets cover the glacial period.

The present day is somewhat well resolved, as about 65 % of the δ^{18}O and δ^{13}C records spanning this time interval exhibit at least ten data points. This trend is also observed for the MH, with about 65 % of the records presenting ten or more data points. δD records appear to be much less well resolved, mostly because a large number of records originate from surface sediment studies based on dated core tops, resulting in a single data point. As a result, only 20 % on the δD records show at least ten data points for the PD. This lower resolution for δD is also verified for the MH, as none of the records present more than ten data points.

Age model quality evaluation

Results from the evaluation of the quality of chronologies are highly variable from marine and lacustrine cores to speleothems (Fig. 7). The overall quality of age models for marine records is moderate. In fact, we note that most of the records published in the 20th century present a missing or crude age model based on an insufficient number of AMS ^{14}C dates, with a lack of reported technical information. Although this result is somewhat deceiving, the quality of age controls has strongly improved during the last 15 years, thanks to better dating technologies and the growing awareness of the absolute necessity to publish robust and well detailed chronologies to precisely reconstruct past climate fluctuations.

Age models in speleothems are much better constrained, as most of the records present an "excellent" or "good" quality flag. Speleothem records are indeed generally constrained by abundant U-Th dates and authors often provide highly detailed technical information. Age anomalies such as age reversals, outliers and hiatuses are nevertheless identified in many records. These anomalies can be caused by analytical issues (e.g. sample contamination, Th adsorption; Musgrove et al., 2011; Wainer et al., 2011) or natural factors occurring simultaneously or after sedimentation process (diagenetic alteration). Hiatuses may be induced by climatic (e.g. severe droughts or permafrost impacts) or post-deposition (e.g. carbonate dissolution) factors (Lachniet, 2009; Breitenbach et al., 2012).

The age models of lacustrine records are relatively good overall, with however larges discrepancies in the quality of chronologies, depending on the dating technique. In fact, some lacustrine records are dated by counting annual/seasonal varves or laminations, leading to an excellent chronology. This dating technique is however generally limited to relatively short records. Records providing longer signals (i.e. spanning several thousand years) are generally dated by AMS ^{14}C dates. Similarly to what is observed for marine core dating, we note the possible lack of technical information in publications, as well as limited resolution of dates, which prevent the establishment of robust age-models. Also, the eventual adjustment applied to ^{14}C ages to correct from radiocarbon reservoir and residence time effects is not systematically provided, as well as the presence of eventual hiatuses.

6.2 Changes between PMIP key periods

δ^{18}O from oceans and atmospheric water (and therefore continental archives) vary in an opposite directions with climate fluctuations. We thus reversed δ^{18}O fluctuations from ocean records in order to map coherent δ^{18}O trends from all the different archives. We however report the original values in the text. We report anomalies with respect to the MH for coherency.

6.2.1 Changes between MH and present-day

The relatively large number of dated δ^{18}O datasets covering both the last 200 years (PD) and the Mid-Holocene (MH) allows us to estimate possible offsets between these two periods (MH-PD; ∼ 100 records from 70 sites; Fig. 8). We restrict the record selection to datasets presenting multiple data points for each of the two periods of interest, thus documenting both the signal (average value) and noise (standard deviation). Results indicate a large dispersion of data, ranging from large positive to negative offsets, while most of the records depict in fact very similar values for the two periods. This feature reflects the spatial heterogeneity of the response to climate changes, making particularly difficult the establishment of large-scale patterns. In a given region, differences also emerge between records from different archives (e.g. opposite sign of changes in speleothem vs. lake records in Eastern Europe). The average difference is low in ice cores, but the overall negative offset observed in ice cores indicates a polar cooling during the last 6 ka, except around the Ross Sea in Antarctica. Particularly remarkable is also the positive anomaly from Chinese speleothems, commonly attributed to changes in Asian summer monsoon with a decrease in rainfall amount through the Holocene (Cai et al., 2010). The standard deviation of the data for the two periods of interest are however quite large in most cases. In fact, in the three types of archives, this noise is either of the same order or higher than the calculated PD-MH offset. As a result, the relatively weak isotopic change between these two periods is not significant in 2/3 of the records. Because we did no account the analytical error associated with δ^{18}O measurements (as this indication was missing in some of the datasets), we may underestimate the noise level, and thus the number of records presenting an insignificant PD-MH offset.

6.2.2 Changes between the last interglacial and MH

We now apply the same approach for the change between LIG and MH (Fig. 9). This relies on 75 δ^{18}O records from ~ 45 sites presenting multiple data points for both of the two periods of interest. We observe more enriched continental (more depleted marine) δ^{18}O values for LIG than during the MH in ~ 20 records, suggesting relatively warmer conditions during LIG, with no apparent geographical trend. However, about half of the LIG-MH anomalies are in the range of the natural standard deviation, and thus cannot be considered as statistically significant. Considering only the records presenting a significant offset nevertheless suggests warmer conditions (enriched continental and depleted marine δ^{18}O) values during the LIG than MH.

Recent syntheses have shown contrasting results in temperature changes between the Last Interglacial period and present day (e.g. Otto-Bliesner et al., 2013), with positive temperature anomalies at both poles, but not occurring simultaneously (Capron et al., 2014), and negative temperature anomalies in some tropical areas. Contrasted regional patterns are expected from the different orbital configurations. Several studies have also highlighted a large magnitude of climate variability during the LIG period (Cheddadi et al., 1998; Lototskaya and Ganssen, 1999; Hearty et al., 2007; Rohling et al., 2007; Pol et al., 2014).

6.2.3 Changes between the LGM and MH

Due to the limited amount of well-dated marine δ^{18}O records covering both the LGM and present day with more than one data point, we compare the LGM and the Mid-Holocene for investigating the isotopic amplitude of last termination (Fig. 10). The LGM-MH comparison reveals a significant negative (positive) offset in almost all the terrestrial (marine) records, with only few speleothem and coral records showing the opposite trend, mostly in the subtropics where they may reflect precipitation or atmospheric circulation effects rather than local temperature variations.

The highest deglacial amplitude is recorded in high elevation and polar ice core records, while the offset is less marked in oceans and speleothems. Marine datasets reveal a latitude-independent general amplitude of ~ 1.45 ‰ (1.55 ‰ when considering only foraminiferal records, with a similar average value for benthics and planktonics), out of which ~ 1 ‰ is due to the change in land ice volume. In addition, we observe specific regional patterns. Larger amplitudes are identified in marine records from the north and South–East Atlantic (about 1.7 ‰), which contrast with smaller amplitudes in the tropics (~ 1.5 ‰) and maximum signals in the Mediterranean Sea (about 2.5 ‰). In this basin, this strong isotopic change is understood to reflect large SSTs deglacial warming and salinity changes induced by shifts in the regional atmospheric circulation (Bigg, 1994; Emeis et al., 2000; Hayes et al., 2005; Mikolajewicz, 2011). Statistics based on benthic foraminiferal δ^{18}O records (including datasets presenting only one data point in the periods of interest) reveal that there is no influence of core site depth on the amplitude of the LGM to MH transition ($R^2 = 0.0029$; $n = 180$).

Ice cores records from high latitudes are all marked by a −3.3 to −7.7 ‰ δ^{18}O shift, with however regional differences such as East–West gradients in both Greenland and Antarctica. Such regional differences may be induced by changes in ice sheet topography and different amplitudes of surface elevation changes at different locations (e.g. Vinther et al., 2009). Similar mechanisms may be at play in Antarctica, but remain poorly documented (e.g. Masson-Delmotte et al., 2011b). There is also evidence for regional differences in the response of Antarctic temperature to climatic changes (Turner et al., 2005; Steig et al., 2009; Steig and Orsi, 2013). The larger amplitude of glacial–interglacial isotopic changes in West Antarctica has been suggested to reflect regional processes coupling the Southern Ocean, sea ice extent and atmospheric heat transport (WAIS Divide Project Members, 2013). It is worth noting that Andean ice cores spanning the last glacial–interglacial transition show a similar deglacial isotopic shift (Vimeux, 2009b). The water stable isotopic composition in those ice cores is likely reflecting precipitation changes at regional scale and such a similar deglacial structure is explained by simultaneous cold conditions in the high latitudes and wetter conditions in the Andes (Vimeux et al., 2005; Chiang and Koutavas, 2008).

Different patterns emerge from speleothem records covering the LGM and MH, as only half of the datasets are marked by a more depleted glacial δ^{18}O level. Depending on the location, speleothem calcite δ^{18}O may reflect either paleotemperature and/or past changes in atmospheric water cycle (including precipitation and circulation). Additional site-specific factors (cave microclimate, mixing and evaporation of source waters through the soil and the epikarst, kinetic fractionation during carbonate precipitation) may also influence the signal (Lachniet, 2009). Regional effects may also be at play in the western Middle East, where speleothem records can be directly influenced by changes in the Mediterranean or the Black Sea, which had diverging oceanographic evolutions between the LGM and the MH, with the opening of the Bosphorus Strait. Individual records must therefore be understood in their own regional environmental context, a feature also evidenced by different amplitudes of change arising from different source archives. Thus, Figs. 8–10 might be considered as an inventory of the available datasets, rather than a cartography of the amplitude of climatically-relevant signals, expected to be representative of the amplitude of annual mean precipitation or sea water isotopic composition changes.

7 Conclusions, recommendations and perspectives

Our compilation of hundreds of records from different sources highlights the needs for a standardized protocol of data storage. The output files provided by the different depositories have different archiving formats. Several ongoing projects rely on massive and automated extraction of datasets provided by authors. This effort would be made easier if the data and publication information (core site specifications, references, article title and abstract) were stored in individual CSV (Comma-Separated Values) text files, rather than within files specifically designed for spreadsheet software (e.g. Microsoft Excel/Apache OpenOffice), sometimes containing several spreadsheets, that may not be readable by automated data extraction programs.

Divergences in data units also constitute a major obstacle for automated extraction, inter-comparison of records, and model-data comparisons. An illustrative example is the use of various time units (years CE, years or before 2000 CE, years before 1950 CE, kiloyears BP, and million years BP). The instauration of standard time units for palaeoclimatology such as use of ka (calendar kiloyears before 1950) would avoid errors and homogenization of future datasets. Several discrepancies also exist with respect to the geographical coordinates of core sites. Although the most common format found in the literature is DMS (Degrees, Minutes, Seconds; e.g.: 25°22′34″ N, 38°16′43″ W), it is not supported by most mapping programs. Here, we converted all the geographical coordinates into decimal degrees. We again highly encourage the adoption of a standard notation, with the systematic presence of the decimal degree version of the coordinates; we observe that an increasing number of authors now provide both DMS and decimal formats.

Gathering information about the age models was a particularly critical step of the construction of this database, in particular for the inclusion of lacustrine and deep sea cores as well as speleothems. There is however no existing standard procedure for the description of age models. The available information is often fragmented, with missing information (raw AMS ^{14}C dates, calibration program/curve used to compute calendar ages, species used for analysis, amount of material measured, marine reservoir ages, tie points, identification of hiatuses in speleothems . . .). A standardized format including all the information related to the establishment of the age models would be a major step forward. We highly encourage the authors to systematically provide both depth and age scales as well as a comprehensive description of the methodology used to establish the age scale, when available. While our earlier comment was centered on deep sea cores, the same features apply for the description of lake sediment cores, ice cores and speleothem chronologies. Even if the methodology developed for the successive chronologies of deep ice cores is usually precisely documented, no standardized reporting protocol exists for ice cores from tropical and temperate glaciers.

We have noticed a clear improvement of the quality of age models and of dating techniques description during the last two decades, and most of the low quality chronologies were published more than 20 years ago. This improvement of age models is particularly critical with respect to the sequences of events during fast transient climate reorganizations. In fact, previous studies have shown that many past major climate changes involved abrupt responses (e.g. de Menocal et al., 2000; Genty et al., 2006; Carlson et al., 2007; Zuraida et al., 2009; Clark et al., 2012; Rach et al., 2014) as well as short delays between different proxy records and regions, like the vigorously debated date and triggering of the onset of Termination I (Schaeffer et al., 2006; Stott et al., 2007; Koutavas and Sachs, 2008; Smith et al., 2008; Bromley et al., 2009; Clark et al., 2009; Shakun et al., 2012; Parrenin et al., 2013). In this context of successive rapid climatic events and keeping in mind the growing interest on performing transient climate simulations, it thus becomes necessary to have a large amount of precisely dated and well defined records. Our database may in the future allow the implementation of statistical age models built on the existing age markers. Reporting the exact number of source records for tree rings and ice cores is also important with respect to the signal to noise issue; this is not always a standard practice.

Our software tool was designed to make the update of the database user-friendly and easy, in order to allow future extension. Indeed, major synthesis efforts as the MARGO project (Waelbroeck et al., 2009) are time limited (MARGO only includes records published prior to 2005). Options for an automatic update include a regular browsing of new published data, but we highly encourage authors to upload their new data in our database using the user-friendly interface on the online platform. This constitutes a fast and easy way to disseminate new data and increase their visibility, and a unique opportunity for the scientific community to access and exploit newly published datasets. This allows "data producers" to easily compare their records with other existing records in a given area or at the global scale, and climate modelers to access easily the data, and to the source references and their authors.

In the future, and if manpower resources are available, the database and web interface could be easily opened to other proxies (paleotemperature proxies and nitrogen isotopes for seawater, CO_2 and CH_4 from ice cores, tree rings width and boreholes, pollens, circulation tracers such as ^{14}C and Pa/Th, etc.) of past and future datasets. We also hope that our database, associated with current and upcoming projects focusing on time-series age control (INTIMATE PROJECT, COST Action ES0907) and chronological data managing (Mulitza and Paul, 2003), would in the future facilitate the use of paleoclimate datasets for data comparison and integration into models with an homogenous and robust chronological frame. This is expected to strengthen the use of proxy information for model-data comparisons, a topic promoted in the Stable Water Isotope Intercomparison group (SWING) and the isotope modeling working group of the Paleoclimate Modelling Intercomparison project, with the potential to better document projections (Schmidt et al., 2014).

Acknowledgements. This study was supported by a national grant from the Agence Nationale de la Recherche under the "Programme d'Investissements d'Avenir" (Grant #ANR-10-LABX-0018) within the framework of LABEX L-IPSL.

References

Ahagon, N.: Mid-depth circulation in the northwest Pacific during the last deglaciation: evidence from foraminiferal radiocarbon ages, Geophys. Res. Lett., 30, 2097, doi:10.1029/2003gl018287, 2003.

Araguas-Araguas, L., Froehlich, K., and Rozanski, K.: Deuterium and oxygen-18 isotope composition of precipitation and atmospheric moisture, Hydrol. Process., 14, 1341–1355, doi:10.1002/1099-1085(20000615)14:8<1341::aid-hyp983>3.0.co;2-z, 2000.

Bakker, P., Masson-Delmotte, V., Martrat, B., Charbit, S., Renssen, H., Gröger, M., Krebs-Kanzow, U., Lohmann, G., Lunt, D. J., Pfeiffer, M., Phipps, S. J., Prange, M., Ritz, S. P., Schulz, M., Stenni, B., Stone, E. J., and Varma, V.: Temperature trends during the Present and Last Interglacial periods – a multi-model-data comparison, Quaternary Sci. Rev., 99, 224–243, doi:10.1016/j.quascirev.2014.06.031, 2014.

Bard, E.: Radiocarbon calibration/comparison records based on marine sediments from the Pakistan and Iberian Margins, Radiocarbon, 55, 1999–2019, doi:10.2458/azu_js_rc.55.17114, 2013.

Barker, S., Broecker, W., Clark, E., and Hajdas, I.: Radiocarbon age offsets of foraminifera resulting from differential dissolution and fragmentation within the sedimentary bioturbated zone, Paleoceanography, 22, PA2205, doi:10.1029/2006pa001354, 2007.

Bar-Matthews, M., Ayalon, A., Gilmour, M., Matthews, A., and Hawkesworth, C. J.: Sea–land oxygen isotopic relationships from planktonic foraminifera and speleothems in the Eastern Mediterranean region and their implication for paleorainfall during interglacial intervals, Geochim. Cosmochim. Ac., 67, 3181–3199, doi:10.1016/s0016-7037(02)01031-1, 2003.

Bazin, L., Landais, A., Lemieux-Dudon, B., Toyé Mahamadou Kele, H., Veres, D., Parrenin, F., Martinerie, P., Ritz, C., Capron, E., Lipenkov, V., Loutre, M.-F., Raynaud, D., Vinther, B., Svensson, A., Rasmussen, S. O., Severi, M., Blunier, T., Leuenberger, M., Fischer, H., Masson-Delmotte, V., Chappellaz, J., and Wolff, E.: An optimized multi-proxy, multi-site Antarctic ice and gas orbital chronology (AICC2012): 120–800 ka, Clim. Past, 9, 1715–1731, doi:10.5194/cp-9-1715-2013, 2013.

Berger, W. H. and Winterer, E. L.: Plate stratigraphy and fluctuating carbonate line, in: Pelagic Sediments on Land and Under the Sea, edited by: Hsü, K. J. and Jenkyns, H. C., International Association of Sedimentologists Special Publication, Oxford, Vol. 1, 11–48, doi:10.1002/9781444304855.ch2, 1974.

Bigg, G. R.: An ocean general circulation model view of the glacial Mediterranean thermohaline circulation, Paleoceanography, 9, 705–722, doi:10.1029/94pa01183, 1994.

Blockley, S. P. E., Lane, C. S., Hardiman, M., Rasmussen, S. O., Seierstad, I., Steffensen, J. P., Svensson, A., Lotter, A. F., Turney, C. S. M., Ramsey, C. B., and INTIMATE members: Synchronisation of palaeoenvironmental records over the last 60,000 years, and an extended INTIMATE event stratigraphy to 48,000 b2k. Quaternary Sci. Rev., 36, 2–10 doi:10.1016/j.quascirev.2011.09.017, 2012.

Bolliet, T., Holbourn, A., Kuhnt, W., Laj, C., Kissel, C., Beaufort, L., Kienast, M., Andersen, N., and Garbe-Schönberg, D.: Mindanao Dome variability over the last 160 kyr: episodic glacial cooling of the West Pacific Warm Pool, Paleoceanography, 26, PA1208, doi:10.1029/2010pa001966, 2011.

Boudreau, B. P.: Mean mixed depth of sediments: the wherefore and the why, Limnol. Oceanogr., 43, 524–526, doi:10.4319/lo.1998.43.3.0524, 1998.

Bouttes, N., Paillard, D., Roche, D. M., Waelbroeck, C., Kageyama, M., Lourantou, A., Michel, E., and Bopp, L.: Impact of oceanic processes on the carbon cycle during the last termination, Clim. Past, 8, 149–170, doi:10.5194/cp-8-149-2012, 2012.

Braconnot, P.: Mid-Holocene and Last Glacial Maximum African monsoon changes as simulated within the Paleoclimate Modelling Intercomparison Project, Global Planet. Change, 26, 51–66, doi:10.1016/s0921-8181(00)00033-3, 2000.

Braconnot, P., Harrison, S. P., Kageyama, M., Bartlein, P. J., Masson-Delmotte, V., Abe-Ouchi, A., Otto-Bliesner, B., and Zhao, Y.: Evaluation of climate models using palaeoclimatic data, Nature Climate Change, 2, 417–424, doi:10.1038/nclimate1456, 2012.

Breitenbach, S. F. M., Rehfeld, K., Goswami, B., Baldini, J. U. L., Ridley, H. E., Kennett, D. J., Prufer, K. M., Aquino, V. V., Asmerom, Y., Polyak, V. J., Cheng, H., Kurths, J., and Marwan, N.: COnstructing Proxy Records from Age models (COPRA), Clim. Past, 8, 1765–1779, doi:10.5194/cp-8-1765-2012, 2012.

Broccoli, A. J., Dahl, K. A., and Stouffer, R. J.: Response of the ITCZ to Northern Hemisphere cooling, Geophys. Res. Lett., 33, L01702, doi:10.1029/2005gl024546, 2006.

Bromley, G. R. M., Schaefer, J. M., Winckler, G., Hall, B. L., Todd, C. E., and Rademaker, K. M.: Relative timing of last glacial maximum and late-glacial events in the central tropical Andes, Quaternary Sci. Rev., 28, 2514–2526, doi:10.1016/j.quascirev.2009.05.012, 2009.

Bronk Ramsey, C., Scott, E. M., and van der Plicht, J.: Calibration for archaeological and environmental terrestrial samples in the time range 26–50 Ka Cal Bp, Radiocarbon, 55, 2021–2027, 2013.

Buizert, C., Gkinis, V., Severinghaus, J. P., He, F., Lecavalier, B. S., Kindler, P., Leuenberger, M., Carlson, A. E., Vinther, B., Masson-Delmotte, V., White, J. W. C., Liu, Z., Otto-Bliesner, B., and Brook, E. J.: Greenland temperature response to climate forcing during the last deglaciation, Science, 345, 1177–1180, doi:10.1126/science.1254961, 2014.

Burke, A. and Robinson, L. F.: The Southern Ocean's role in carbon exchange during the last deglaciation, Science, 335, 557–561, doi:10.1126/science.1208163, 2011.

Cai, Y., Tan, L., Cheng, H., An, Z., Edwards, R., Kelly, M., Kong, X., and Wang, X.: The variation of summer monsoon precipitation in central China since the last deglaciation, Earth Planet. Sci. Lett., 291, 21–31, 2010.

Caley, T. and Roche, D. M.: δ^{18}O water isotope in the *i*LOVECLIM model (version 1.0) – Part 3: A palaeo-perspective based on present-day data–model comparison for oxygen stable isotopes in carbonates, Geosci. Model Dev., 6, 1505–1516, doi:10.5194/gmd-6-1505-2013, 2013.

Caley, T., Roche, D. M., Waelbroeck, C., and Michel, E.: Oxygen stable isotopes during the Last Glacial Maximum climate: perspectives from data–model (*i*LOVECLIM) comparison, Clim. Past, 10, 1939–1955, doi:10.5194/cp-10-1939-2014, 2014.

Capron, E., Govin, A., Stone, E. J., Masson-Delmotte, V., Mulitza, S., Otto-Bliesner, B., Rasmussen, T. L., Sime, L. C., Waelbroeck, C., and Wolff, E. W.: Temporal and spatial structure of multi-millennial temperature changes at high latitudes during the Last Interglacial, Quaternary Sci. Rev., 103, 116–133, doi:10.1016/j.quascirev.2014.08.018, 2014.

Carlson, A. E., Clark, P. U., Raisbeck, G. M., and Brook, E. J.: Rapid Holocene deglaciation of the Labrador Sector of the Laurentide Ice Sheet, J. Climate, 20, 5126–5133, doi:10.1175/jcli4273.1, 2007.

Carré, M., Azzoug, M., Bentaleb, I., Chase, B. M., Fontugne, M., Jackson, D., Ledru, M.-P., Maldonado, A., Sachs, J. P., and Schauer, A. J.: Mid-Holocene mean climate in the south eastern Pacific and its influence on South America, Quatern. Int., 253, 55–66, doi:10.1016/j.quaint.2011.02.004, 2012.

Cheddadi, R., Lamb, H. F., Guiot, J., and van der Kaars, S.: Holocene climatic change in Morocco: a quantitative reconstruction from pollen data, Clim. Dynam., 14, 883–890, doi:10.1007/s003820050262, 1998.

Chiang, J. C. H. and Koutavas, A.: Climate change: tropical flip-flop connections, Nature, 432, 684–685, 2004.

Chylek, P., Lesins, G., and Lohmann, U.: Enhancement of dust source area during past glacial periods due to changes of the Hadley circulation, J. Geophys. Res., 106, 18477, doi:10.1029/2000jd900583, 2001.

Clark, C. D., Hughes, A. L. C., Greenwood, S. L., Jordan, C., and Sejrup, H. P.: Pattern and timing of retreat of the last British-Irish Ice Sheet, Quaternary Sci. Rev., 44, 112–146, doi:10.1016/j.quascirev.2010.07.019, 2012.

Clark, P. U., Dyke, A. S., Shakun, J. D., Carlson, A. E., Clark, J., Wohlfarth, B., Mitrovica, J. X., Hostetler, S. W., and McCabe, A. M.: The Last Glacial Maximum, Science, 325, 710–714, doi:10.1126/science.1172873, 2009.

Collins, M., Knutti, R., Arblaster, J., Dufresne, J.-L., Fichefet, T., Friedlingstein, P., Gao, X., Gutowski, W. J., Johns, T., Krinner, G., Shongwe, M., Tebaldi, C., Weaver, A. J., and Wehner, M.: Long-term climate change: projections, commitments and irreversibility, in: Climate Change 2013: The Physical ScienceBasis. Contribution of Working Group I to the Fifth Assessment Report of the Intergovernmental Panel on Climate Change, edited by: Stocker, T. F., Qin, D., Plattner, G.-K., Tignor, M., Allen, S. K., Boschung, J., Nauels, A., Xia, Y., Bex, V., and Midgley, P. M., Cambridge University Press, Cambridge, UK and New York, NY, USA, 1029–1136, doi:10.1017/CBO9781107415324.024, 2013.

Cruz, F. W., Burns, S. J., Karmann, I., Sharp, W. D., and Vuille, M.: Reconstruction of regional atmospheric circulation features during the late Pleistocene in subtropical Brazil from oxygen isotope composition of speleothems, Earth Planet. Sc. Lett., 248, 495–507, doi:10.1016/j.epsl.2006.06.019, 2006.

Csank, A. Z.: An international tree-ring isotope data bank – a proposed repository for tree-ring isotopic data, Tree-Ring Res., 65, 163–164, doi:10.3959/1536-1098-65.2.163, 2009.

Dahl-Jensen, D., Albert, M. R., Aldahan, A., Azuma, N., Balslev-Clausen, D., Baumgartner, M., Berggren, A. M., Bigler, M., Binder, T., Blunier, T., Bourgeois, J. C., Brook, E. J., Buchardt, S. L., Buizert, C., Capron, E., Chappellaz, J., Chung, J., Clausen, H. B., Cvijanovic, I., Davies, S. M., Ditlevsen, P., Eicher, O., Fischer, H., Fisher, D. A., Fleet, L. G., Gfeller, G., Gkinis, V., Gogineni, S., Goto-Azuma, K., Grinsted, A., Gudlaugsdottir, H., Guillevic, M., Hansen, S. B., Hansson, M., Hirabayashi, M., Hong, S., Hur, S. D., Huybrechts, P., Hvidberg, C. S., Iizuka, Y., Jenk, T., Johnsen, S. J., Jones, T. R., Jouzel, J., Karlsson, N. B., Kawamura, K., Keegan, K., Kettner, E., Kipfstuhl, S., Kjær, H. A., Koutnik, M., Kuramoto, T., Köhler, P., Laepple, T., Landais, A., Langen, P. L., Larsen, L. B., Leuenberger, D., Leuenberger, M., Leuschen, C., Li, J., Lipenkov, V., Martinerie, P., Maselli, O. J., Masson-Delmotte, V., McConnell, J. R., Miller, H., Mini, O., Miyamoto, A., Montagnat-Rentier, M., Mulvaney, R., Muscheler, R., Orsi, A. J., Paden, J., Panton, C., Pattyn, F., Petit, J. R., Pol, K., Popp, T., Possnert, G., Prié, F., Prokopiou, M., Quiquet, A., Rasmussen, S. O., Raynaud, D., Ren, J., Reutenauer, C., Ritz, C., Röckmann, T., Rosen, J. L., Rubino, M., Rybak, O., Samyn, D., Sapart, C. J., Schilt, A., Schmidt, A. M. Z., Schwander, J., Schüpbach, S., Seierstad, I., Severinghaus, J. P., Sheldon, S., Simonsen, S. B., Sjolte, J., Solgaard, A. M., Sowers, T., Sperlich, P., Steen-Larsen, H. C., Steffen, K., Steffensen, J. P., Steinhage, D., Stocker, T. F., Stowasser, C., Sturevik, A. S., Sturges, W. T., Sveinbjörnsdottir, A., Svensson, A., Tison, J. L., Uetake, J., Vallelonga, P., van de Wal, R. S. W., van der Wel, G., Vaughn, B. H., Vinther, B., Waddington, E., Wegner, A., Weikusat, I., White, J. W. C., Wilhelms, F., Winstrup, M., Witrant, E., Wolff, E. W., Xiao, C., and Zheng, J.: Eemian interglacial reconstructed from a Greenland folded ice core, Nature, 493, 489–494, doi:10.1038/nature11789, 2013.

Daux, V., Edouard, J. L., Masson-Delmotte, V., Stievenard, M., Hoffmann, G., Pierre, M., Mestre, O., Danis, P. A., and Guibal, F.: Can climate variations be inferred from tree-ring parameters and stable isotopes from Larix decidua? Juvenile effects, budmoth outbreaks, and divergence issue, Earth Planet. Sc. Lett., 309, 221–233, doi:10.1016/j.epsl.2011.07.003, 2011.

deMenocal, P., Ortiz, J., Guilderson, T., Adkins, J., Sarnthein, M., Baker, L., and Yarusinsky, M.: Abrupt onset and termination of the African Humid Period, Quaternary Sci. Rev., 19, 347–361, doi:10.1016/s0277-3791(99)00081-5, 2000.

Duplessy, J. C., Shackleton, N. J., Fairbanks, R. G., Labeyrie, L., Oppo, D., and Kallel, N.: Deepwater source variations during the last climatic cycle and their impact on the global deepwater circulation, Paleoceanography, 3, 343–360, 1988.

Ehleringer, J. R. and Vogel, J. C.: Historical aspects of stable isotopes in plant carbon and water relations, in: Stable Isotopes and Plant Carbon/Water Relations, edited by: Ehleringer, J. R., Hall, A. E., and Farquhar, G. D., Academic Press, San Diego, p. 9–18, 1993.

Emeis, K.-C., Struck, U., Schulz, H.-M., Rosenberg, R., Bernasconi, S., Erlenkeuser, H., Sakamoto, T., and Martinez-Ruiz, F.: Temperature and salinity variations of Mediterranean Sea surface waters over the last 16,000 years from records of planktonic stable oxygen isotopes and alkenone unsaturation ratios, Palaeogeogr. Palaeocl., 158, 259–280, doi:10.1016/s0031-0182(00)00053-5, 2000.

Fallet, U., Castañeda, I. S., Henry-Edwards, A., Richter, T. O., Boer, W., Schouten, S., and Brummer, G.-J.: Sedimentation and burial of organic and inorganic temperature proxies in the Mozambique Channel, SW Indian Ocean, Deep-Sea Res. Pt. I, 59, 37–53, doi:10.1016/j.dsr.2011.10.002, 2012.

Fisher, D. A.: Stratigraphic noise in time series derives from ice cores, Ann. Glaciol., 7, 76–83, 1985.

Flato, G., Marotzke, J., Abiodun, B., Braconnot, P., Chou, S. C., Collins, W., Cox, P., Driouech, F., Emori, S., Eyring, V., Forest, C., Gleckler, P., Guilyardi, E., C.Jakob, Kattsov, V., Reason and Rummukainen, C., M.: Evaluation of climate models, in: Climate Change 2013: The Physical Science Basis. Contribution of Working Group I to the Fifth Assessment Report of the Intergovernmental Panel on Climate Change, edited by: Stocker, T. F., Qin, D., Plattner, G.-K., Tignor, M., Allen, S. K., Boschung, J., Nauels, A., Xia, Y., Bex, V., and Midgley, P. M., Cambridge University Press, Cambridge, UK and New York, NY, USA, 741–866, doi:10.1017/CBO9781107415324.020, 2013.

Fudge, T. J., Steig, E. J., Markle, B. R., Schoenemann, S. W., Ding, Q., Taylor, K. C., McConnell, J. R., Brook, E. J., Sowers, T., White, J. W. C., Alley, R. B., Cheng, H., Clow, G. D., Cole-Dai, J., Conway, H., Cuffey, K. M., Edwards, J. S., Lawrence Edwards, R., Edwards, R., Fegyveresi, J. M., Ferris, D., Fitzpatrick, J. J., Johnson, J., Hargreaves, G., Lee, J. E., Maselli, O. J., Mason, W., McGwire, K. C., Mitchell, L. E., Mortensen, N., Neff, P., Orsi, A. J., Popp, T. J., Schauer, A. J., Severinghaus, J. P., Sigl, M., Spencer, M. K., Vaughn, B. H., Voigt, D. E., Waddington, E. D., Wang, X., and Wong, G. J.: Onset of deglacial warming in West Antarctica driven by local orbital forcing, Nature, 500, 440–444, doi:10.1038/nature12376, 2013.

Genty, D., Blamart, D., Ghaleb, B., Plagnes, V., Causse, C., Bakalowicz, M., Zouari, K., Chkir, N., Hellstrom, J., and Wainer, K.: Timing and dynamics of the last deglaciation from European and North African δ13C stalagmite profiles – comparison with Chinese and South Hemisphere stalagmites, Quaternary Sci. Rev., 25, 2118–2142, doi:10.1016/j.quascirev.2006.01.030, 2006.

Govin, A., Braconnot, P., Capron, E., Cortijo, E., Duplessy, J.-C., Jansen, E., Labeyrie, L., Landais, A., Marti, O., Michel, E., Mosquet, E., Risebrobakken, B., Swingedouw, D., and Waelbroeck, C.: Persistent influence of ice sheet melting on high northern latitude climate during the early Last Interglacial, Clim. Past, 8, 483–507, doi:10.5194/cp-8-483-2012, 2012.

Grant, K. M., Rohling, E. J., Bar-Matthews, M., Ayalon, A., Medina-Elizalde, M., Ramsey, C. B., Satow, C., and Roberts, A. P.: Rapid coupling between ice volume and polar temperature over the past 150,000 years, Nature, 491, 744–747, doi:10.1038/nature11593, 2012.

Grant, K. M., Rohling, E. J., Ramsey, C. B., Cheng, H., Edwards, R. L., Florindo, F., Heslop, D., Marra, F., Roberts, A. P., Tamisiea, M. E., and Williams, F.: Sea-level variability over five glacial cycles, Nature Communications, 5, 5076, doi:10.1038/ncomms6076, 2014.

Guillevic, M., Bazin, L., Landais, A., Kindler, P., Orsi, A., Masson-Delmotte, V., Blunier, T., Buchardt, S. L., Capron, E., Leuenberger, M., Martinerie, P., Prié, F., and Vinther, B. M.: Spatial gradients of temperature, accumulation and δ^{18}O-ice in Greenland over a series of Dansgaard–Oeschger events, Clim. Past, 9, 1029–1051, doi:10.5194/cp-9-1029-2013, 2013.

Harrison, S. P., Bartlein, P. J., Brewer, S., Prentice, I. C., Boyd, M., Hessler, I., Holmgren, K., Izumi, K., and Willis, K.: Climate model benchmarking with glacial and mid-Holocene climates, Clim. Dynam., 43, 671–688, doi:10.1007/s00382-013-1922-6, 2013.

Hayes, A., Kucera, M., Kallel, N., Sbaffi, L., and Rohling, E. J.: Glacial Mediterranean sea surface temperatures based on planktonic foraminiferal assemblages, Quaternary Sci. Rev., 24, 999–1016, doi:10.1016/j.quascirev.2004.02.018, 2005.

Hearty, P. J., Hollin, J. T., Neumann, A. C., O'Leary, M. J., and McCulloch, M.: Global sea-level fluctuations during the Last Interglaciation (MIS 5e), Quaternary Sci. Rev., 26, 2090–2112, doi:10.1016/j.quascirev.2007.06.019, 2007.

Henderson-Sellers, A., Fischer, M., Aleinov, I., McGuffie, K., Riley, W. J., Schmidt, G. A., Sturm, K., Yoshimura, K., and Irannejad, P.: Stable water isotope simulation by current land-surface schemes: results of iPILPS Phase 1, Global Planet. Change, 51, 34–58, doi:10.1016/j.gloplacha.2006.01.003, 2006.

Hughen, K., Southon, J., Lehman, S., Bertrand, C., and Turnbull, J.: Marine-derived 14C calibration and activity record for the past 50,000 years updated from the Cariaco Basin, Quaternary Sci. Rev., 25, 3216–3227, doi:10.1016/j.quascirev.2006.03.014, 2006.

IAEA/WMO: Global Network of Isotopes in Precipitation. The GNIP Database, available at: http://www.iaea.org/water (last access: July 2015), 2015.

IPCC: Climate Change 2013: The Physical Science Basis. Contribution of Working Group I to the Fifth Assessment Report of the Intergovernmental Panel on Climate Change, edited by: Stocker, T. F., Qin, D., Plattner, G.-K., Tignor, M., Allen, S. K., Boschung, J., Nauels, A., Xia, Y., Bex, V., and Midgley, P. M., Cambridge University Press, Cambridge, UK and New York, NY, USA, 1535 pp., doi:10.1017/CBO9781107415324, 2013.

Jasechko, S., Lechler, A., Pausata, F. S. R., Fawcett, P. J., Gleeson, T., Cendón, D. I., Galewsky, J., LeGrande, A. N., Risi, C., Sharp, Z. D., Welker, J. M., Werner, M., and Yoshimura, K.: Glacial–interglacial shifts in global and regional precipitation δ^{18}O, Clim. Past Discuss., 11, 831–872, doi:10.5194/cpd-11-831-2015, 2015.

Joussaume, S., Sadourny, R., and Jouzel, J.: A general circulation model of water isotope cycles in the atmosphere, Nature, 311, 24–29, doi:10.1038/311024a0, 1984.

Justino, F. and Peltier, W. R.: The glacial North Atlantic Oscillation, Geophys. Res. Lett., 32, L21803, doi:10.1029/2005gl023822, 2005.

Keigwin, L. D. and Guilderson, T. P.: Bioturbation artifacts in zero-age sediments, Paleoceanography, 24, PA4212, doi:10.1029/2008pa001727, 2009.

Kohfeld, K. E. and Chase, Z.: Controls on deglacial changes in biogenic fluxes in the North Pacific Ocean, Quaternary Sci. Rev., 30, 3350–3363, doi:10.1016/j.quascirev.2011.08.007, 2011.

Koutavas, A. and Sachs, J. P.: Northern timing of deglaciation in the eastern equatorial Pacific from alkenone paleothermometry, Paleoceanography, 23, PA4205, doi:10.1029/2008pa001593, 2008.

Kukla, G. J., Bender, M. L., Beaulieu, J.-L. de, Bond, G., Broecker, W. S., Cleveringa, P., Gavin, J. E., Herbert, T. D., Imbrie, J., Jouzel, J., Keigwin, L. D., Knudsen, K.-L., McManus, J. F., Merkt, J., Muhs, D. R., Müller, H., Poore, R. Z., Porter, S., Seret, G., Shakleton, N. J., Turner, C., and Winograd, I. J.: Last Interglacial, Climates Quaternary Res., 58, 2–13, 2002.

Labuhn, I., Daux, V., Pierre, M., Stievenard, M., Girardclos, O., Féron, A., Genty, D., Masson-Delmotte, V., and Mestre, O.: Tree age, site and climate controls on tree ring cellulose δ^{18}O: a case study on oak trees from south-western France, Dendrochronologia, 32, 78–89, doi:10.1016/j.dendro.2013.11.001, 2014.

Lachniet, M. S.: Climatic and environmental controls on speleothem oxygen-isotope values, Quaternary Sci. Rev., 28, 412–432, doi:10.1016/j.quascirev.2008.10.021, 2009.

Leduc, G., Vidal, L., Tachikawa, K., and Bard, E.: ITCZ rather than ENSO signature for abrupt climate changes across the tropical Pacific?, Quaternary Res., 72, 123–131, doi:10.1016/j.yqres.2009.03.006, 2009.

Lee, J.-E., Risi, C., Fung, I., Worden, J., Scheepmaker, R. A., Lintner, B., and Frankenber, C.: Asian monsoon hydrometeorology from TES and SCIAMACHY water vapor isotope measurements and LMDZ simulations: implications for speleothem climate record interpretation, J. Geophys. Res., 117, D15112, doi:10.1029/2011JD017133, 2012.

Libby, L. M. and Pandolfi, L. J.: Isotopic tree thermometers: correlation with radiocarbon, J. Geophys. Res., 81, 6377–6381, doi:10.1029/JC081i036p06377, 1976.

Long, A.: Stable isotopes in tree rings, in: Climate From Tree Rings, edited by: Hughes, M. K., Kelly, P. M., Pilcher, J. R., and LaMarche, V. C.: Cambridge University Press, Cambridge, 13–18, 1982.

Lototskaya, A. and Ganssen, G. M.: The structure of Termination II (penultimate deglaciation and Eemian) in the North Atlantic, Quaternary Sci. Rev., 18, 1641–1654, doi:10.1016/s0277-3791(99)00011-6, 1999.

Lunt, D. J., Abe-Ouchi, A., Bakker, P., Berger, A., Braconnot, P., Charbit, S., Fischer, N., Herold, N., Jungclaus, J. H., Khon, V. C., Krebs-Kanzow, U., Langebroek, P. M., Lohmann, G., Nisancioglu, K. H., Otto-Bliesner, B. L., Park, W., Pfeiffer, M., Phipps, S. J., Prange, M., Rachmayani, R., Renssen, H., Rosenbloom, N., Schneider, B., Stone, E. J., Takahashi, K., Wei, W., Yin, Q., and Zhang, Z. S.: A multi-model assessment of last interglacial temperatures, Clim. Past, 9, 699–717, doi:10.5194/cp-9-699-2013, 2013.

Lwemark, L., Jakobsson, M., Mrth, M., and Backman, J.: Arctic Ocean manganese contents and sediment colour cycles, Polar Res., 27, 105–113, doi:10.1111/j.1751-8369.2008.00055.x, 2008.

Marcott, S. A., Shakun, J. D., Clark, P. U., and Mix, A. C.: A reconstruction of regional and global temperature for the past 11,300 years, Science, 339, 1198–1201, doi:10.1126/science.1228026, 2013.

Masson-Delmotte, V., Stenni, B., Blunier, T., Cattani, O., Chappellaz, J., Cheng, H., Dreyfus, G., Edwards, R. L., Falourd, S., Govin, A., Kawamura, K., Johnsen, S. J., Jouzel, J., Landais, A., Lemieux-Dudon, B., Lourantou, A., Marshall, G., Minster, B., Mudelsee, M., Pol, K., Rothlisberger, R., Selmo, E., and Waelbroeck, C.: Abrupt change of Antarctic moisture origin at the end of Termination II, P. Natl. Acad. Sci. USA, 107, 12091–12094, doi:10.1073/pnas.0914536107, 2010.

Masson-Delmotte, V., Braconnot, P., Hoffmann, G., Jouzel, J., Kageyama, M., Landais, A., Lejeune, Q., Risi, C., Sime, L., Sjolte, J., Swingedouw, D., and Vinther, B.: Sensitivity of interglacial Greenland temperature and δ^{18}O: ice core data, orbital and increased CO_2 climate simulations, Clim. Past, 7, 1041–1059, doi:10.5194/cp-7-1041-2011, 2011a.

Masson-Delmotte, V., Buiron, D., Ekaykin, A., Frezzotti, M., Gallée, H., Jouzel, J., Krinner, G., Landais, A., Motoyama, H., Oerter, H., Pol, K., Pollard, D., Ritz, C., Schlosser, E., Sime, L. C., Sodemann, H., Stenni, B., Uemura, R., and Vimeux, F.: A comparison of the present and last interglacial periods in six Antarctic ice cores, Clim. Past, 7, 397–423, doi:10.5194/cp-7-397-2011, 2011b.

Masson-Delmotte, V., Schulz, M., Abe-Ouchi, A., Beer, J., Ganopolski, J., González Rouco, J. F., Jansen, E., Lambeck, K., Luterbacher, J., Naish, T., Osborn, T., Otto-Bliesner, B., Quinn, T., Ramesh, R., Rojas, M., Shao, X., and Timmermann, A.: Information from paleoclimate archives, in: Climate Change 2013: The Physical Science Basis. Contribution of Working Group I to the Fifth Assessment Report of the Intergovernmental Panel on Climate Change, edited by: Stocker, T. F., Qin, D., Plattner, G.-K., Tignor, M., Allen, S. K., Doschung, J., Nauels, A., Xia, Y., Bex, V., and Midgley, P. M., Cambridge University Press, Cambridge, UK, 383–464, doi:10.1017/CBO9781107415324.013, 2013.

Masson-Delmotte, V., Steen-Larsen, H. C., Ortega, P., Swingedouw, D., Popp, T., Vinther, B. M., Oerter, H., Sveinbjornsdottir, A. E., Gudlaugsdottir, H., Box, J. E., Falourd, S., Fettweis, X., Gallée, H., Garnier, E., Gkinis, V., Jouzel, J., Landais, A., Minster, B., Paradis, N., Orsi, A., Risi, C., Werner, M., and White, J. W. C.: Recent changes in north-west Greenland climate documented by NEEM shallow ice core data and simulations, and implications for past-temperature reconstructions, The Cryosphere, 9, 1481–1504, doi:10.5194/tc-9-1481-2015, 2015.

Max, L., Lembke-Jene, L., Riethdorf, J.-R., Tiedemann, R., Nürnberg, D., Kühn, H., and Mackensen, A.: Pulses of enhanced North Pacific Intermediate Water ventilation from the Okhotsk Sea and Bering Sea during the last deglaciation, Clim. Past, 10, 591–605, doi:10.5194/cp-10-591-2014, 2014.

McCarroll, D. and Loader, N. J.: Stable isotopes in tree rings, Quaternary Sci. Rev., 23, 771–801, doi:10.1016/j.quascirev.2003.06.017, 2004.

Menviel, L., Joos, F., and Ritz, S. P.: Simulating atmospheric CO2, 13C and the marine carbon cycle during the Last Glacial–Interglacial cycle: possible role for a deepening of the mean remineralization depth and an increase in the oceanic nutrient inventory, Quaternary Sci. Rev., 56, 46–68, doi:10.1016/j.quascirev.2012.09.012, 2012.

Mikolajewicz, U.: Modeling Mediterranean Ocean climate of the Last Glacial Maximum, Clim. Past, 7, 161–180, doi:10.5194/cp-7-161-2011, 2011.

Mix, A. C., Lund, D. C., Pisias, N. G., Bodén, P., Bornmalm, L., Lyle, M., and Pike, J.: Rapid climate oscillations in the Northeast Pacific during the last deglaciation reflect, Northern and Southern Hemisphere Sources, 112, 127–148, doi:10.1029/GM112p0127, 1999.

Mulitza, S. and Paul, A.: A GUI-based synthesis toolbox for the collection, homogenization and visualization of foraminiferal stable isotope data, PMIP Ocean Workshop 2013: Understanding Changes since the Last Glacial Maximum, Corvallis, Oregon, USA, 4–6 December 2013.

Murakami, S., Ohgaito, R., Abe-Ouchi, A., Crucifix, M., and Otto-Bliesner, B. L.: Global-scale energy and freshwater balance in glacial climate: a comparison of three PMIP2 LGM simulations, J. Climate, 21, 5008–5033, doi:10.1175/2008jcli2104.1, 2008.

Musgrove, M., Banner, J. L., Mack, L. E., Combs, D. M., James, E. W., Cheng, H., and Edwards, R. L.: Geochronology of late Pleistocene to Holocene speleothems from central Texas: Implications for regional paleoclimate, Geol. Soc. Am. Bull., 113, 1532–1543, doi::10.1130/0016-7606(2001)113<1532:GOLPTH>2.0.CO;2, 2001.

Nikolova, I., Yin, Q., Berger, A., Singh, U. K., and Karami, M. P.: The last interglacial (Eemian) climate simulated by LOVECLIM and CCSM3, Clim. Past, 9, 1789–1806, doi:10.5194/cp-9-1789-2013, 2013.

Oppo, D. W., Schmidt, G. A., and LeGrande, A. N.: Seawater isotope constraints on tropical hydrology during the Holocene, Geophys. Res. Lett., 34, L13701, doi:10.1029/2007gl030017, 2007.

Otto-Bliesner, B. L., Rosenbloom, N., Stone, E. J., McKay, N. P., Lunt, D. J., Brady, E. C., and Overpeck, J. T.: How warm was the last interglacial? New model-data comparisons, Philos. T. R. Soc. A, 371, 20130097, doi:10.1098/rsta.2013.0097, 2013.

Parrenin, F., Masson-Delmotte, V., Kohler, P., Raynaud, D., Paillard, D., Schwander, J., Barbante, C., Landais, A., Wegner, A., and Jouzel, J.: Synchronous change of atmospheric CO_2 and antarctic temperature during the last deglacial warming, Science, 339, 1060–1063, doi:10.1126/science.1226368, 2013.

Plastino, W. and Bella, F.: Radon groundwater monitoring at underground laboratories of Gran Sasso (Italy), Geophys. Res. Lett., 28, 2675–2677, doi:10.1029/2000gl012430, 2001.

Pol, K., Masson-Delmotte, V., Cattani, O., Debret, M., Falourd, S., Jouzel, J., Landais, A., Minster, B., Mudelsee, M., Schulz, M., and Stenni, B.: Climate variability features of the last interglacial in the East Antarctic EPICA Dome C ice core, Geophys. Res. Lett., 41, 4004–4012, doi:10.1002/2014gl059561, 2014.

Rach, O., Brauer, A., Wilkes, H., and Sachse, D.: Delayed hydrological response to Greenland cooling at the onset of the Younger Dryas in western Europe, Nat. Geosci., 7, 109–112, doi:10.1038/ngeo2053, 2014.

Rasmussen, S. O., Andersen, K. K., Svensson, A. M., Steffensen, J. P., Vinther, B. M., Clausen, H. B., Siggaard-Andersen, M. L., Johnsen, S. J., Larsen, L. B., Dahl-Jensen, D., Bigler, M., Röthlisberger, R., Fischer, H., Goto-Azuma, K., Hansson, M. E., and Ruth, U.: A new Greenland ice core chronology for the last glacial termination, J. Geophys. Res., 111, D06102, doi:10.1029/2005jd006079, 2006.

Reimer, P.: IntCal13 and Marine13 radiocarbon age calibration curves 0–50,000 years cal BP, Radiocarbon, 55, 1869–1887, doi:10.2458/azu_js_rc.55.16947, 2013.

Richter, S. L., Johnson, A. H., Dranoff, M. M., LePage, B. A., and Williams, C. J.: Oxygen isotope ratios in fossil wood cellulose: isotopic composition of Eocene- to Holocene-aged cellulose, Geochim. Cosmochim. Ac., 72, 2744–2753, doi:10.1016/j.gca.2008.01.031, 2008.

Risi, C., Bony, S., Vimeux, F., and Jouzel, J.: Water-stable isotopes in the LMDZ4 general circulation model: model evaluation for present-day and past climates and applications to climatic interpretations of tropical isotopic records, J. Geophys. Res., 115, D12118, doi:10.1029/2009jd013255, 2010.

Roche, D. M. and Caley, T.: δ^{18}O water isotope in the *i*LOVECLIM model (version 1.0) – Part 2: Evaluation of model results against observed δ^{18}O in water samples, Geosci. Model Dev., 6, 1493–1504, doi:10.5194/gmd-6-1493-2013, 2013.

Rohling, E. J., Grant, K., Hemleben, C., Siddall, M., Hoogakker, B. A. A., Bolshaw, M., and Kucera, M.: High rates of sea-level rise during the last interglacial period, Nat. Geosci., 1, 38–42, doi:10.1038/ngeo.2007.28, 2007.

Rohling, E. J., Rohling, E. J., Sluijs, A., Dijkstra, H. A., Köhler, P., van de Wal, R. S. W., von der Heydt, A. S., Beerling, D. J., Berger, A., Bijl, P. K., Crucifix, M., DeConto, R., Drijfhout, S. S., Fedorov, A., Foster, G. L., Ganopolski, A., Hansen, J., Hönisch, B., Hooghiemstra, H., Huber, M., Huybers, P., Knutti, R., Lea, D. W., Lourens, L. J., Lunt, D., Masson-Demotte, V., Medina-Elizalde, M., Otto-Bliesner, B., Pagani, M., Pälike, H., Renssen, H., Royer, D. L., Siddall, M., Valdes, P., Zachos, J. C., and Zeebe, R. E.: Making sense of palaeoclimate sensitivity, Nature, 491, 683–691, doi:10.1038/nature11574, 2012.

Ruth, U., Barnola, J.-M., Beer, J., Bigler, M., Blunier, T., Castellano, E., Fischer, H., Fundel, F., Huybrechts, P., Kaufmann, P., Kipfstuhl, S., Lambrecht, A., Morganti, A., Oerter, H., Parrenin, F., Rybak, O., Severi, M., Udisti, R., Wilhelms, F., and Wolff, E.: "EDML1": a chronology for the EPICA deep ice core from Dronning Maud Land, Antarctica, over the last 150 000 years, Clim. Past, 3, 475–484, doi:10.5194/cp-3-475-2007, 2007.

Sarnthein, M., Winn, K., Duplessy, J.-C., and Fontugne, M.: Global variations of surface ocean productivity in low and mid latitudes: influence on CO_2 reservoirs of the deep ocean and atmosphere during the last 21,000 years, Paleoceanography, 3, 361–399, doi:10.1029/PA003i003p00361, 1988.

Sarnthein, M., Winn, K., Jung, S. J. A., Duplessy, J.-C., Labeyrie, L., Erlenkeuser, H., and Ganssen, G.: Changes in East Atlantic deepwater circulation over the last 30,000 years: eight time slice reconstructions, Paleoceanography, 9, 209–267, doi:10.1029/93pa03301, 1994.

Schaefer, J. M.: Near-synchronous interhemispheric termination of the Last Glacial Maximum in mid-latitudes, Science, 312, 1510–1513, doi:10.1126/science.1122872, 2006.

Schmidt, G. A., LeGrande, A. N., and Hoffmann, G.: Water isotope expressions of intrinsic and forced variability in a coupled ocean–atmosphere model, J. Geophys. Res., 112, D10103, doi:10.1029/2006jd007781, 2007.

Schmidt, G. A., Annan, J. D., Bartlein, P. J., Cook, B. I., Guilyardi, E., Hargreaves, J. C., Harrison, S. P., Kageyama, M., LeGrande, A. N., Konecky, B., Lovejoy, S., Mann, M. E., Masson-Delmotte, V., Risi, C., Thompson, D., Timmermann, A., Tremblay, L.-B., and Yiou, P.: Using palaeo-climate comparisons to constrain future projections in CMIP5, Clim. Past, 10, 221–250, doi:10.5194/cp-10-221-2014, 2014.

Shakun, J. D., Clark, P. U., He, F., Marcott, S. A., Mix, A. C., Liu, Z., Otto-Bliesner, B., Schmittner, A., and Bard, E.: Global warming preceded by increasing carbon dioxide concentrations during the last deglaciation, Nature, 484, 49–54, doi:10.1038/nature10915, 2012.

Shin, S.-I.: Southern Ocean sea-ice control of the glacial North Atlantic thermohaline circulation, Geophys. Res. Lett., 30, 1096, doi:10.1029/2002gl015513, 2003.

Siani, G., Michel, E., De Pol-Holz, R., DeVries, T., Lamy, F., Carel, M., Isguder, G., Dewilde, F., and Lourantou, A.: Carbon isotope records reveal precise timing of enhanced Southern Ocean upwelling during the last deglaciation, Nature Communications, 4, 2758, doi:10.1038/ncomms3758, 2013.

Sime, L. C., Wolff, E. W., Oliver, K. I. C., and Tindall, J. C.: Evidence for warmer interglacials in East Antarctic ice cores, Nature, 462, 342–345, doi:10.1038/nature08564, 2009.

Sime, L. C., Risi, C., Tindall, J. C., Sjolte, J., Wolff, E. W., Masson-Delmotte, V., and Capron, E.: Warm climate isotopic simulations: What do we learn about interglacial signals in Greenland ice cores?, Quaternary Sci. Rev., 67, 59–80, doi:10.1016/j.quascirev.2013.01.009, 2013.

Skinner, L. C., Fallon, S., Waelbroeck, C., Michel, E., and Barker, S.: Ventilation of the deep Southern Ocean and deglacial CO_2 rise, Science, 328, 1147–1151, doi:10.1126/science.1183627, 2010.

Smith, J. A., Mark, B. G., and Rodbell, D. T.: The timing and magnitude of mountain glaciation in the tropical Andes, J. Quaternary Sci., 23, 609–634, doi:10.1002/jqs.1224, 2008.

Sortor, R. N. and Lund, D. C.: No evidence for a deglacial intermediate water Δ14C anomaly in the SW Atlantic, Earth Planet. Sc. Lett., 310, 65–72, doi:10.1016/j.epsl.2011.07.017, 2011.

Soulet, G., Ménot, G., Garreta, V., Rostek, F., Zaragosi, S., Lericolais, G., and Bard, E.: Black Sea “Lake” reservoir age evolution since the Last Glacial – Hydrologic and climatic implications, Earth Planet. Sc. Lett., 308, 245–258, doi:10.1016/j.epsl.2011.06.002, 2011.

Sperling, M., Schmiedl, G., Hemleben, C., Emeis, K. C., Erlenkeuser, H., and Grootes, P. M.: Black Sea impact on the formation of eastern Mediterranean sapropel S1? Evidence from the Marmara Sea, Palaeogeogr. Palaeocl., 190, 9–21, doi:10.1016/s0031-0182(02)00596-5, 2003.

Sprowl, D. R.: On the precision of the Elk Lake varve chronology, in: Elk Lake, Minnesota: Evidence for Rapid Climate Change in the North-Central United States, edited by: Bradbury, J. P., Geological Society of America, Boulder, CO, Special Paper 276, 69–74, 1993.

Steig, E. J. and Orsi, A. J.: Climate Science: the heat is on in Antarctica, Nat. Geosci., 6, 87–88, doi:10.1038/ngeo1717, 2013.

Steig, E. J., Schneider, D. P., Rutherford, S. D., Mann, M. E., Comiso, J. C., and Shindell, D. T.: Warming of the Antarctic ice-sheet surface since the 1957 International Geophysical Year, Nature, 457, 459–462, doi:10.1038/nature07669, 2009.

Sternberg, L. d. S. L. O. R.: Oxygen stable isotope ratios of tree-ring cellulose: the next phase of understanding, New Phytol., 181, 553–562, doi:10.1111/j.1469-8137.2008.02661.x, 2009.

Stocker, T. F.: The Seesaw Effect, Science, 282, 61–62, doi:10.1126/science.282.5386.61, 1998.

Stott, L.: Super ENSO and global climate oscillations at millennial time scales, Science, 297, 222–226, doi:10.1126/science.1071627, 2002.

Stott, L., Timmermann, A., and Thunell, R.: Southern Hemisphere and deep-sea warming led deglacial atmospheric CO_2 rise and tropical warming, Science, 318, 435–438, doi:10.1126/science.1143791, 2007.

Stuiver, M. and Braziunas, T. F.: Tree cellulose 13C/12C isotope ratios and climatic change, Nature, 328, 58–60, doi:10.1038/328058a0, 1987.

Sturm, C., Zhang, Q., and Noone, D.: An introduction to stable water isotopes in climate models: benefits of forward proxy modelling for paleoclimatology, Clim. Past, 6, 115–129, doi:10.5194/cp-6-115-2010, 2010.

Sun, Y., Oppo, D. W., Xiang, R., Liu, W., and Gao, S.: Last deglaciation in the Okinawa Trough: subtropical northwest Pacific link to Northern Hemisphere and tropical climate, Paleoceanography, 20, PA4005, doi:10.1029/2004pa001061, 2005.

Switsur, R. and Waterhouse, J.: Stable isotopes in tree ring cellulose, in: Stable Isotopes: Integration of Biological, Ecological and Geochemical Processes, edited by: Griffiths, H., BIOS Scientific Publishers Ltd., Oxford, 303–321, 1998.

Sylvestre, F.: Moisture pattern during the last glacial maximum in South America in Past climate variability from the Last Glacial Maximum to the Holocene in South America an Surrounding regions, in: Developments in Paleoenvironmental Research Series (DPER), edited by: Vimeux, F., Sylvestre, F., and Khodri, M., Springer, New York, Vol. 14, XVII, 418 p. 106 illus., 61 in color., ISBN 978-90-481-2671-2, 2009.

Tagliabue, A., Bopp, L., Roche, D. M., Bouttes, N., Dutay, J.-C., Alkama, R., Kageyama, M., Michel, E., and Paillard, D.: Quantifying the roles of ocean circulation and biogeochemistry in governing ocean carbon-13 and atmospheric carbon dioxide at the last glacial maximum, Clim. Past, 5, 695–706, doi:10.5194/cp-5-695-2009, 2009.

Tessin, A. C. and Lund, D. C.: Isotopically depleted carbon in the mid-depth South Atlantic during the last deglaciation, Paleoceanography, 28, 296–306, doi:10.1002/palo.20026, 2013.

Tindall, J. C., Valdes, P. J., and Sime, L. C.: Stable water isotopes in HadCM3: isotopic signature of El Niño–Southern Oscillation and the tropical amount effect, J. Geophys. Res., 114, D04111, doi:10.1029/2008jd010825, 2009.

Tudhope, A. W.: Variability in the El Niño–Southern Oscillation through a glacial–interglacial cycle, Science, 291, 1511–1517, doi:10.1126/science.1057969, 2001.

Turner, J., Colwell, S. R., Marshall, G. J., Lachlan-Cope, T. A., Carleton, A. M., Jones, P. D., Lagun, V., Reid, P. A., and Iagovkina, S.: Antarctic climate change during the last 50 years, Int. J. Climatol., 25, 279–294, doi:10.1002/joc.1130, 2005.

Van Campo, E.: Monsoon fluctuations in two 20,000-Yr B.P. oxygen-isotope/pollen records off southwest India, Quaternary Res., 26, 376–388, doi:10.1016/0033-5894(86)90097-9, 1986.

Veres, D., Bazin, L., Landais, A., Toyé Mahamadou Kele, H., Lemieux-Dudon, B., Parrenin, F., Martinerie, P., Blayo, E., Blunier, T., Capron, E., Chappellaz, J., Rasmussen, S. O., Severi, M., Svensson, A., Vinther, B., and Wolff, E. W.: The Antarctic ice core chronology (AICC2012):

an optimized multi-parameter and multi-site dating approach for the last 120 thousand years, Clim. Past, 9, 1733–1748, doi:10.5194/cp-9-1733-2013, 2013.

Vimeux, F., Gallaire, R., Bony, S., Hoffmann, G., Chiang. J., and Fuertes, R.: What are the climate controls on isotopic composition (dD) of precipitation in Zongo Valley (Bolivia) ? Implications for the Illimani ice core interpretation, Earth Planet. Sc. Lett., 240, 205–220, 2005.

Vimeux, F., de Angelis, M., Ginot, P., Magand, O., Pouyaud, B., Casassa, G., Johnsen, S., Falourd, S.: A promising location in Patagonia for paleoclimate and environmental reconstructions revealed by a shallow firn core from Monte San Valentin (Northern Patagonia Icefield, Chile), J. Geophys. Res., 113, D16118, doi:10.1029/2007JD009502, 2008.

Vimeux, F., Ginot, P., Schwikowski, M., Vuille, M., Hoffmann, G., Thompson, L. G., and Schotterer, U.: Climate variability during the last 1000 years inferred from Andean ice cores: a review of methodology and recent results, Palaeogeogr. Palaeocl., 281, 229–241, doi:10.1016/j.palaeo.2008.03.054, 2009a.

Vimeux, F.: Similarities and discrepancies between Polar and Andean ice cores over the last deglaciation in Past climate variability from the Last Glacial Maximum to the Holocene in South America an Surrounding regions, in: Developments in Paleoenvironmental Research Series (DPER), edited by: Vimeux, F., Sylvestre, F., and Khodri, M., Springer, New York, Vol. 14, XVII, 418 p. 106 illus., 61 in color., ISBN 978-90-481-2671-2, 2009b.

Vinther, B. M., Clausen, H. B., Johnsen, S. J., Rasmussen, S. O., Andersen, K. K., Buchardt, S. L., Dahl-Jensen, D., Seierstad, I. K., Siggaard-Andersen, M. L., Steffensen, J. P., Svensson, A., Olsen, J., and Heinemeier, J.: A synchronized dating of three Greenland ice cores throughout the Holocene, J. Geophys. Res., 111, D13102, doi:10.1029/2005jd006921, 2006.

Vinther, B. M., Buchardt, S. L., Clausen, H. B., Dahl-Jensen, D., Johnsen, S. J., Fisher, D. A., Koerner, R. M., Raynaud, D., Lipenkov, V., Andersen, K. K., Blunier, T., Rasmussen, S. O., Steffensen, J. P., and Svensson, A. M.: Holocene thinning of the Greenland ice sheet, Nature, 461, 385–388, doi:10.1038/nature08355, 2009.

Waelbroeck, C., Paul, A., Kucera, M., Rosell-Melé, A., Weinelt, M., Schneider, R., Mix, A. C., Abelmann, A., Armand, L., Bard, E., Barker, S., Barrows, T. T., Benway, H., Cacho, I., Chen, M. T., Cortijo, E., Crosta, X., de Vernal, A., Dokken, T., Duprat, J., Elderfield, H., Eynaud, F., Gersonde, R., Hayes, A., Henry, M., Hillaire-Marcel, C., Huang, C. C., Jansen, E., Juggins, S., Kallel, N., Kiefer, T., Kienast, M., Labeyrie, L., Leclaire, H., Londeix, L., Mangin, S., Matthiessen, J., Marret, F., Meland, M., Morey, A. E., Mulitza, S., Pflaumann, U., Pisias, N. G., Radi, T., Rochon, A., Rohling, E. J., Sbaffi, L., Schäfer-Neth, C., Solignac, S., Spero, H., Tachikawa, K., and Turon, J. L.: Constraints on the magnitude and patterns of ocean cooling at the Last Glacial Maximum, Nat. Geosci., 2, 127–132, doi:10.1038/ngeo411, 2009.

Wainer, K., Genty, D., Blamart, D., Daëron, M., Bar-Matthews, M., Vonhof, H., Dublyansky, Y., Pons-Branchu, E., Thomas, L., van Calsteren, P., Quinif, Y., and Caillon, N.: Speleothem record of the last 180 ka in Villars cave (SW France): investigation of a large δ18O shift between MIS6 and MIS5, Quaternary Sci. Rev., 30, 130–146, doi:10.1016/j.quascirev.2010.07.004, 2011.

Wang, Y. J., Cheng, H., Edwards, R. L., An, Z. S., Wu, J. Y., Shen, C. C., and Dorale, J. A.: A high-resolution absolute-dated late Pleistocene Monsoon record from Hulu Cave, China, Science, 294, 2345–2348, doi:10.1126/science.1064618, 2001.

Wang, Y. J., Cheng, H., Edwards, R. L., He, Y. Q., Kong, X. G., An, Z. S., Wu, J. Y., Kelly, M. J., Dykoski, C. A., and Li, X. D.: The Holocene Asian Monsoon: links to solar changes and North Atlantic climate, Science, 308, 854–857, 2005.

Weldeab, S., Schneider, R. R., and Kölling, M.: Deglacial sea surface temperature and salinity increase in the western tropical Atlantic in synchrony with high latitude climate instabilities, Earth Planet. Sc. Lett., 241, 699–706, doi:10.1016/j.epsl.2005.11.012, 2006.

Werner, M., Langebroek, P. M., Carlsen, T., Herold, M., and Lohmann, G.: Stable water isotopes in the ECHAM5 general circulation model: toward high-resolution isotope modeling on a global scale, J. Geophys. Res., 116, D15109, doi:10.1029/2011jd015681, 2011.

Yoshimura, K., Miyazaki, S., Kanae, S., and Oki, T.: Iso-MATSIRO, a land surface model that incorporates stable water isotopes, Global Planet. Change, 51, 90–107, doi:10.1016/j.gloplacha.2005.12.007, 2006.

Yoshimura, K., Kanamitsu, M., Noone, D., and Oki, T.: Historical isotope simulation using Reanalysis atmospheric data, J. Geophys. Res., 113, D19108, doi:10.1029/2008jd010074, 2008.

Yoshimura, K., Frankenberg, C., Lee, J., Kanamitsu, M., Worden, J., and Röckmann, T.: Comparison of an isotopic atmospheric general circulation model with new quasi-global satellite measurements of water vapor isotopologues, J. Geophys. Res., 116, D19118, doi:10.1029/2011jd016035, 2011.

Yu, E.-F., Francois, R., and Bacon, M. P.: Similar rates of modern and last-glacial ocean thermohaline circulation inferred from radiochemical data, Nature, 379, 689–694, doi:10.1038/379689a0, 1996.

Yuan, D., Cheng, H., Edwards, R. L., Dykoski, C. A., Kelly, M. J., Zhang, M., Qing, J., Lin, Y., Wang, Y., Wu, J., Dorale, J. A., An, Z., and Cai, Y.: Last interglacial Asian Monsoon, Science, 304, 575–578, 2004.

Zuraida, R., Holbourn, A., Nürnberg, D., Kuhnt, W., Dürkop, A., and Erichsen, A.: Evidence for Indonesian throughflow slowdown during Heinrich events 3–5, Paleoceanography, 24, PA2205, doi:10.1029/2008pa001653, 2009.

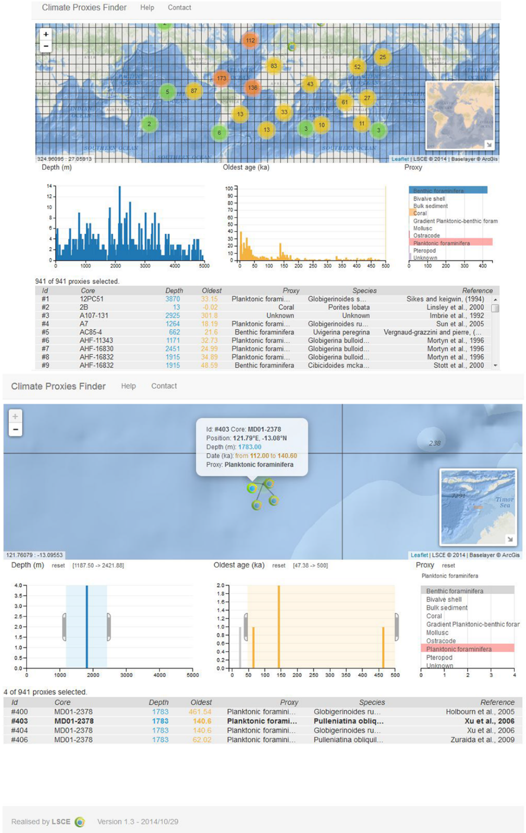

941 of 941 proxies selected.

Id	Core	Depth	Oldest	Proxy	Species	Reference
#1	12PC51	3870	33.15	Planktonic forami...	Globigerinoides s...	Sikes and keigwin, (1994)
#2	2B	13	-0.02	Coral	Porites lobata	Linsley et al., 2000
#3	A107-131	2925	301.8	Unknown	Unknown	Imbrie et al., 1992
#4	A7	1264	18.19	Planktonic forami...	Globigerinoides ru...	Sun et al., 2005
#5	AC85-4	662	21.6	Benthic foraminifera	Uvigerina peregrina	Vergnaud-grazzini and pierre, (...
#6	AHF-11343	1171	32.73	Planktonic forami...	Globigerina bulloid...	Mortyn et al., 1996
#7	AHF-16830	2451	24.99	Planktonic forami...	Globigerina bulloid...	Mortyn et al., 1996
#8	AHF-16832	1915	34.89	Planktonic forami...	Globigerina bulloid...	Mortyn et al., 1996
#9	AHF-16832	1915	48.59	Benthic foraminifera	Cibicidoides mcka...	Stott et al., 2000

Id: **#403** Core: **MD01-2378**
Position: **121.79°E, -13.08°N**
Depth (m): **1783.00**
Date (ka): from **112.00** to **140.60**
Proxy: **Planktonic foraminifera**

4 of 941 proxies selected.

Id	Core	Depth	Oldest	Proxy	Species	Reference
#400	MD01-2378	1783	461.54	Planktonic foramini...	Globigerinoides ru...	Holbourn et al., 2005
#403	**MD01-2378**	**1783**	**140.6**	**Planktonic forami...**	**Pulleniatina obliq...**	**Xu et al., 2006**
#404	MD01-2378	1783	140.6	Planktonic foramini...	Globigerinoides ru...	Xu et al., 2006
#406	MD01-2378	1783	62.02	Planktonic foramini...	Pulleniatina obliquil...	Zuraida et al., 2009

Figure 1. Web portal screen captures illustrating the search criteria (top) and the resulting maps (bottom).

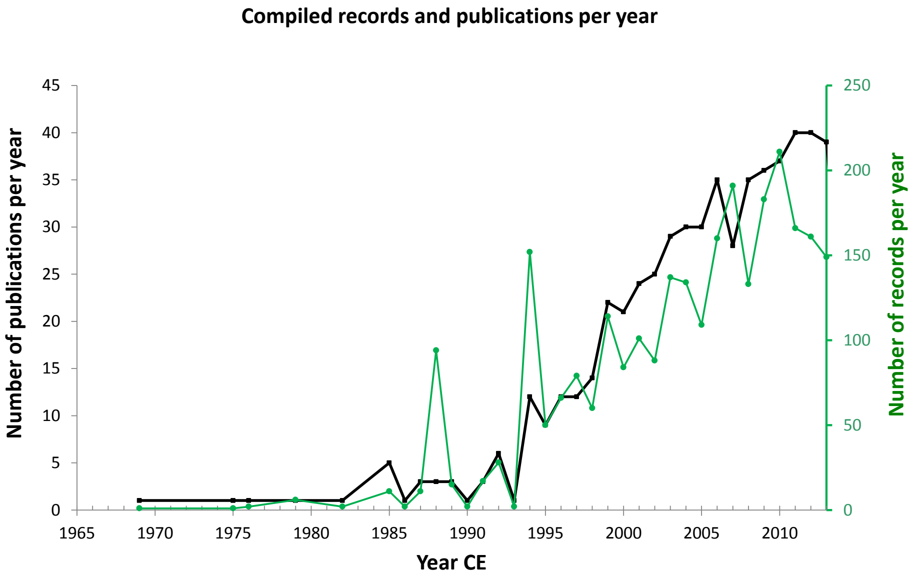

Figure 2. Number of publications and records in the database vs. year of publication.

Title Page
Abstract
Introduction
Conclusions
References
Tables
Figures
I◀
▶I
◀
▶
Back
Close
Full Screen / Esc
Printer-friendly Version
Interactive Discussion

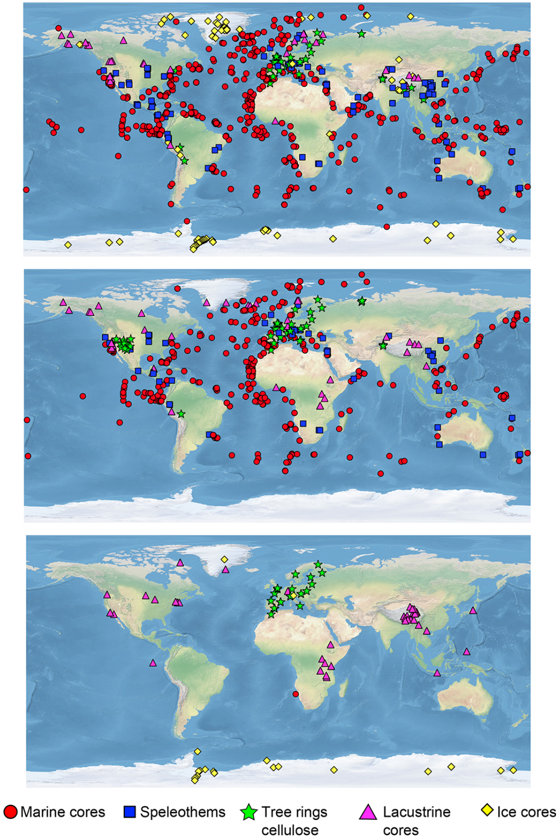

Figure 3. Map indicating the position of archives with different symbols representing the type of archive for dated δ^{18}O (top) δ^{13}C (center) and δD records (bottom) available on the online portal. Note that these maps only display the location of dated records, and stack and multi-sites composite records are not included.

Title Page
Abstract | Introduction
Conclusions | References
Tables | Figures
I◀ | ▶I
◀ | ▶
Back | Close
Full Screen / Esc
Printer-friendly Version
Interactive Discussion

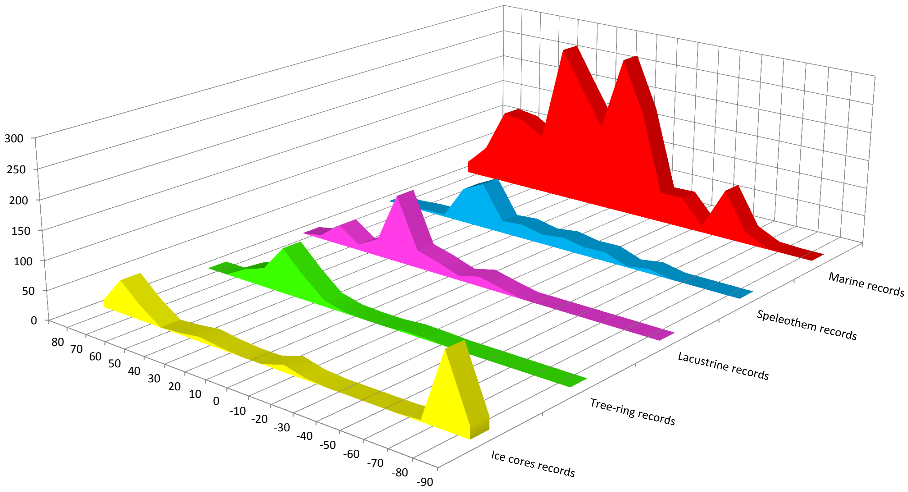

Figure 4. Diagram showing the distribution of ice cores, tree-ring, lacustrine, speleothem and marine records as a function of latitude (°).

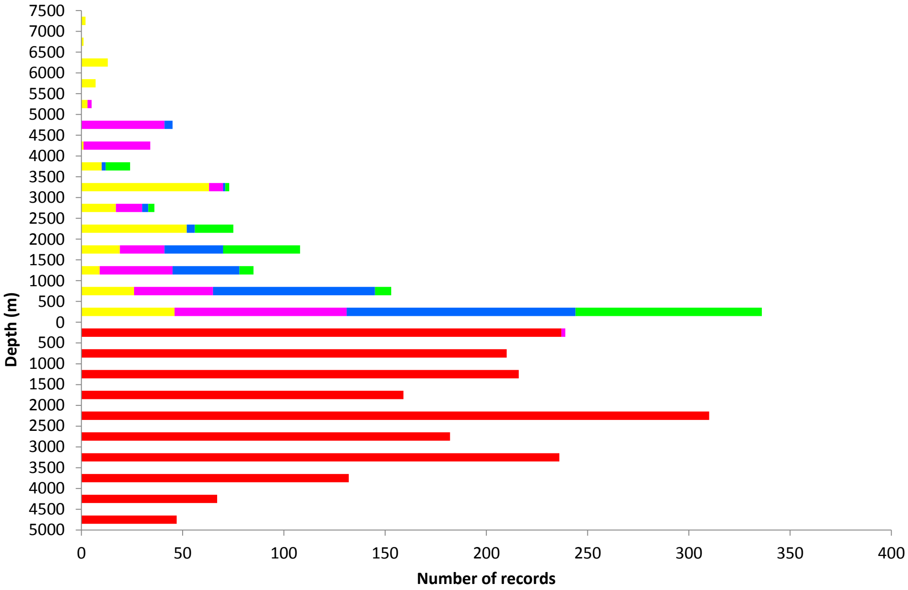

Figure 5. Diagram showing the distribution of ice cores, tree-ring, lacustrine, speleothem and marine records as a function of coring site elevation.

Title Page
Abstract
Introduction
Conclusions
References
Tables
Figures
◀
▶
Back
Close
Full Screen / Esc
Printer-friendly Version
Interactive Discussion

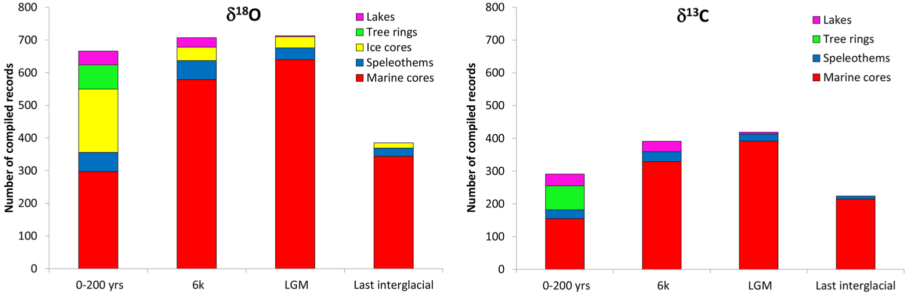

Figure 6. Diagrams showing the number of δ^{18}O and δ^{13}C records from marine and lake cores, speleothems, ice cores, and tree ring cellulose for each PMIP time slice.

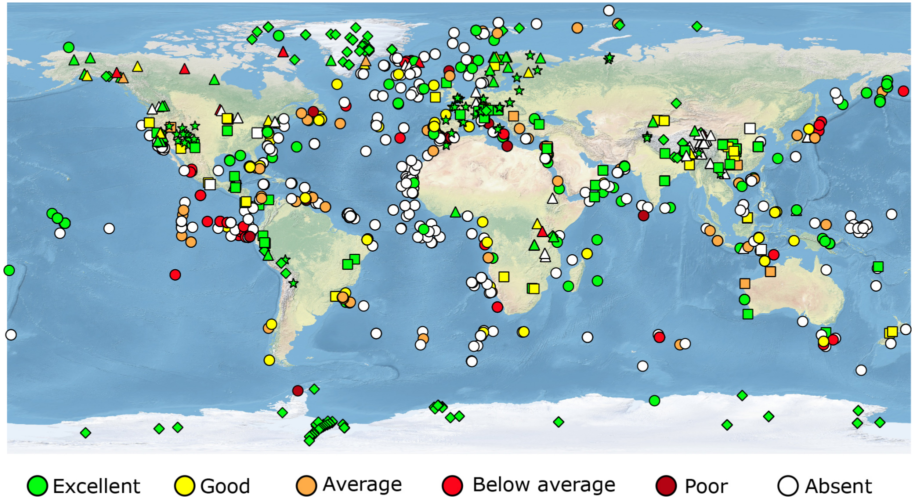

Figure 7. Location of lacustrine (triangles), speleothems (squares) and marine records (circles) where chronological information is available, and with quality flags for age model quality evaluation.

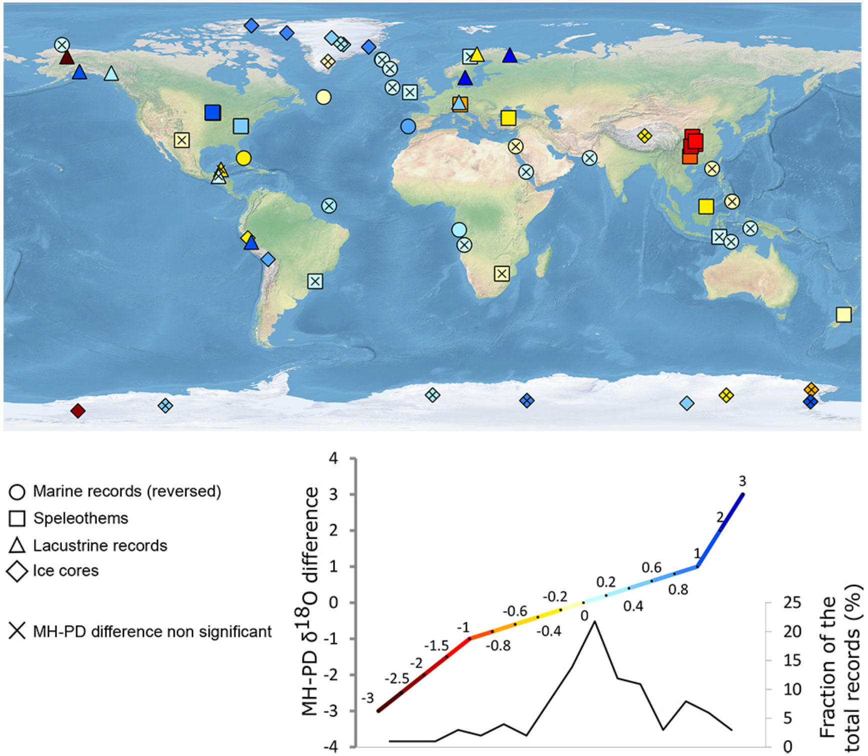

Figure 8. Map showing the location of δ^{18}O records spanning the MH and PD with the symbols reflecting the type of source archive and colors documenting the amplitude of δ^{18}O variations between these two periods (MH-PD). The bottom figure shows the color scale as well as the fraction of records as a function of the MH-PD δ^{18}O anomaly. Note the non-linear scale for δ^{18}O difference. The δ^{18}O difference from marine records was reversed for coherency with the sign of changes of terrestrial records. Note that some proximate core-sites may not be visible on the figure because of graphical overlaps.

CPD

doi:10.5194/cp-2015-165

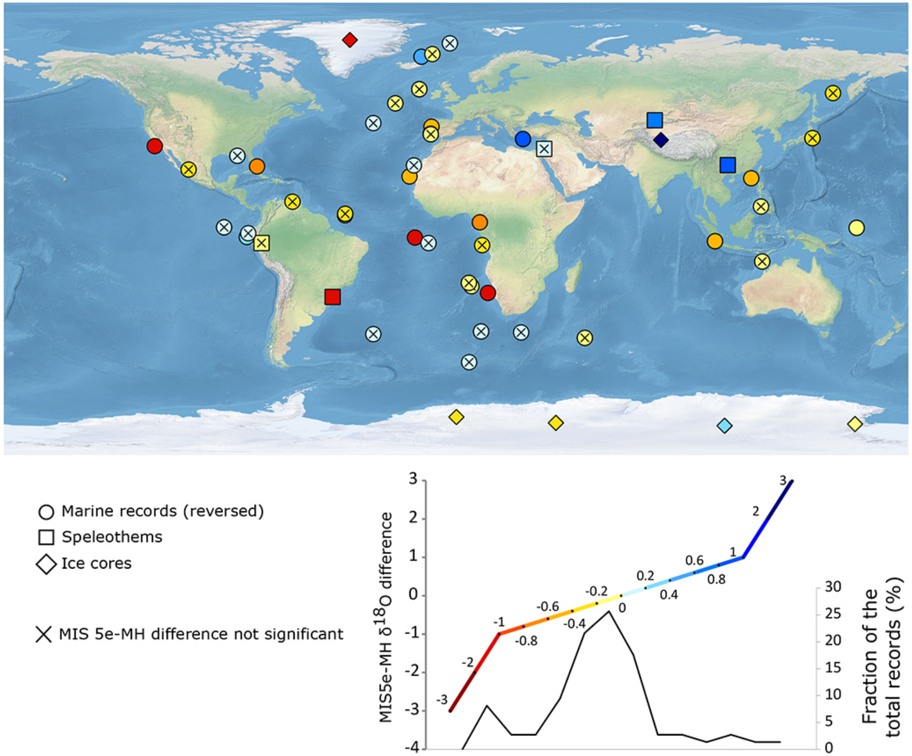

Figure 9. Same as Fig. 8 but for the difference between LIG and MH values (LIG-MH).

CPD

doi:10.5194/cp-2015-165

Title Page
Abstract | Introduction
Conclusions | References
Tables | Figures
|◀ | ▶|
◀ | ▶
Back | Close
Full Screen / Esc
Printer-friendly Version
Interactive Discussion

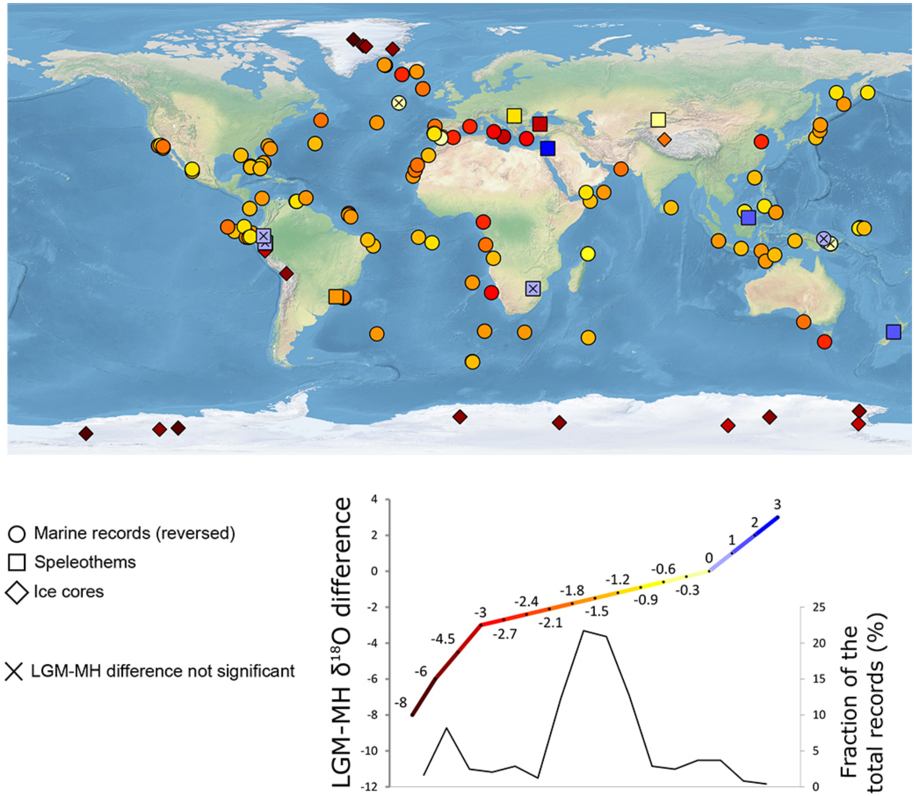

Figure 10. Same as Fig. 8 but between the MH and the LGM (LGM-MH).

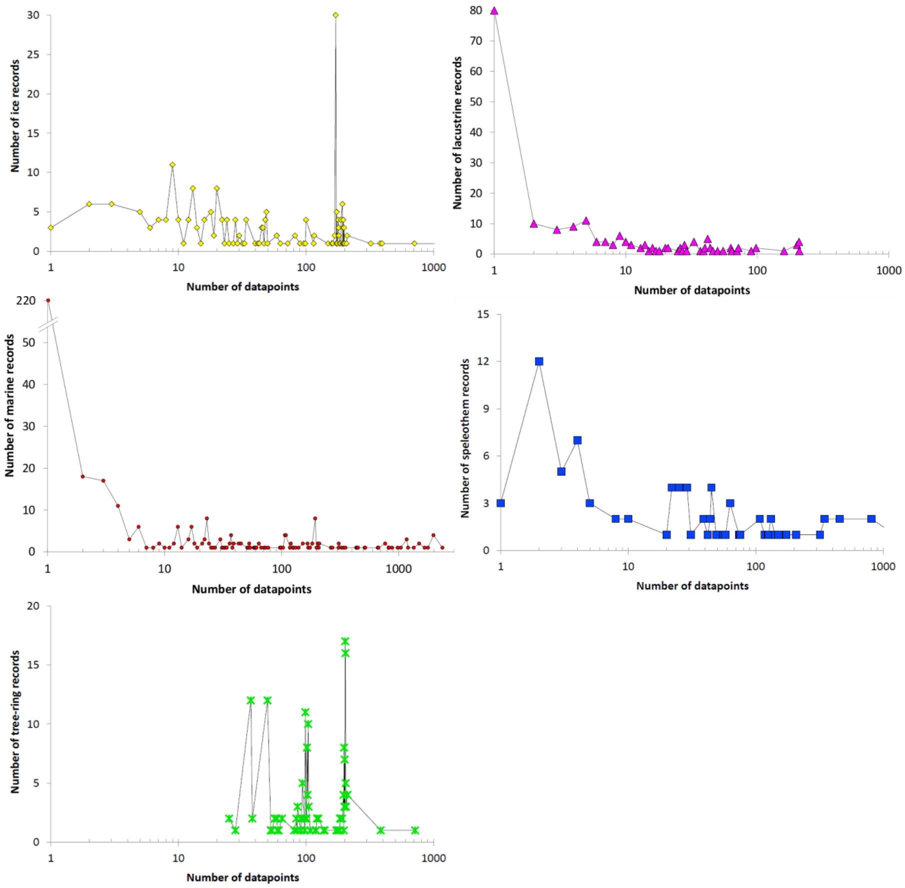

Figure A1. Diagrams showing the distribution of records (number of records) as a function of their mean time resolution (number of data points) for the different types of archives compiled in the database for the Present day (18:00–20:13 CE). Note the different vertical scales.

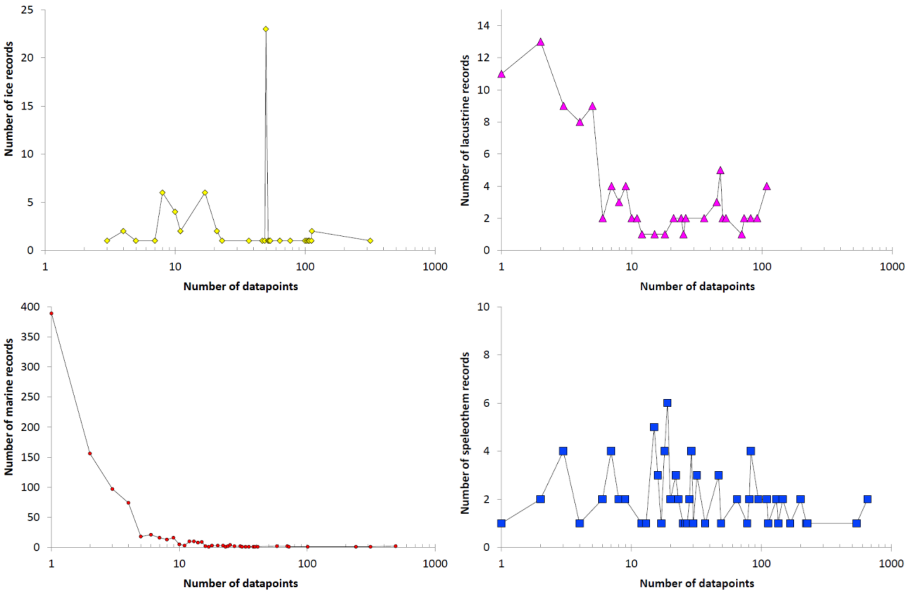

Figure A2. Same as Fig. 1 but for the Mid-Holocene (5.5–6.5 ka). Note the different vertical scales.

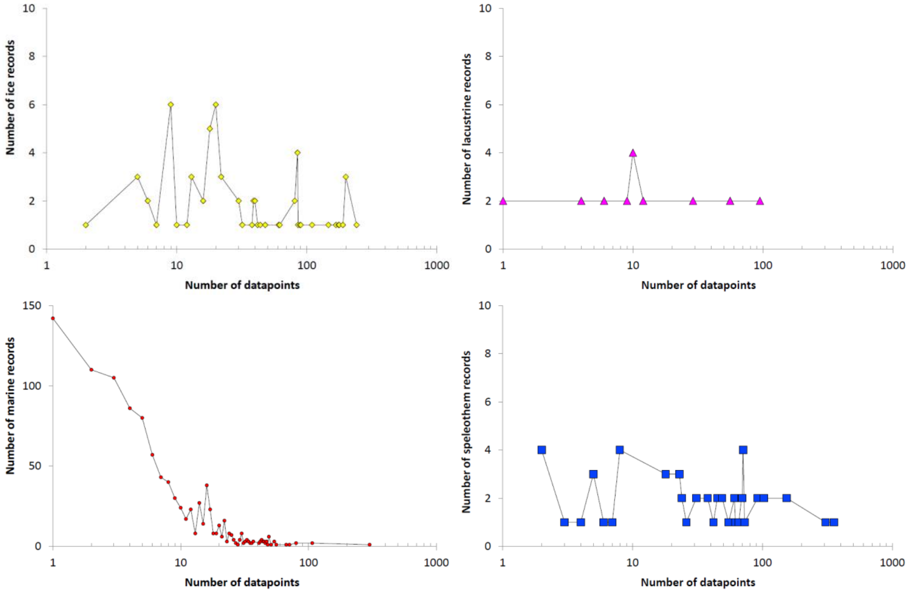

Figure A3. Same as Fig. 1 but for the LGM (19–23 ka). Note the different vertical scales.

Title Page
Abstract Introduction
Conclusions References
Tables Figures
◀ ▶
Back Close
Full Screen / Esc
Printer-friendly Version
Interactive Discussion

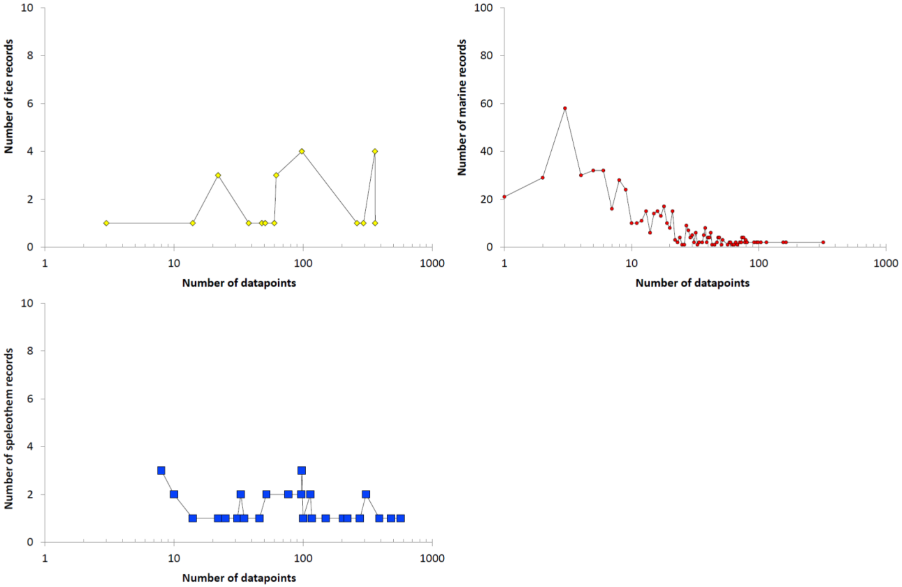

Figure A4. Same as Fig. 1 but for the last Interglacial (115–130 ka). Note the different vertical scales.